

# UC San Diego

## UC San Diego Previously Published Works

### Title

New archaeointensity results from Scandinavia and Bulgaria Rock-magnetic studies inference and geophysical application

### Permalink

<https://escholarship.org/uc/item/7w25x0fm>

### Journal

Physics of the Earth and Planetary Interiors, 165

### ISSN

0031-9201

### Authors

Donadini, F.  
Kostadinova, M.  
Pesonen, L. J.  
[et al.](#)

### Publication Date

2007-12-01

### DOI

10.1016/j.pepi.2007.10.002

Peer reviewed

This study investigates archaeological artifacts from five sites in Europe: one from Switzerland (Cheyres - baked clay remains from an Iron Age kiln: 700-530BC); one from Bulgaria (Drustur - Medieval kiln: 1200-1300AD); two from Finland (Busö - Medieval kiln: 1570AD and bricks from Helsinki: 1906AD); and one from Russian Karelia (bricks from Valaam: 1856AD).

The goal of the paper is to determine palaeointensity from the archaeological sites mentioned above, as well as to compare the values obtained in different laboratories.

Palaeointensity experiments were mainly carried out at the Division of Geophysics, University of Helsinki and at the Palaeomagnetic Laboratory of the Geophysical Institute in Sofia. Additionally, microwave palaeointensity determinations on few sister specimens from Helsinki bricks and from Drustur kiln were performed in Liverpool. Large amount of rock-magnetic studies accompanies the work in order to find possible explanations for the acceptance or failure of palaeointensity experiments. The encountered difficulties in obtaining reliable palaeointensity results are discussed and show a still incomplete state of art for determination of this important ancient geomagnetic field characteristic.

The accepted new palaeointensity evaluations for different time and space will partly fill up considerable gaps in European palaeointensity databases. Geophysical inference is demonstrated on the basis of virtual axial dipole moment calculated from the new palaeointensity results and its relationship with the CALS7K.2 model calculation and the observatory measurements for the corresponding territories.

**New archaeointensity results from Scandinavia and Bulgaria. Rock-magnetic studies inference and geophysical application.**

F. Donadini <sup>a,b\*</sup>, M. Kovacheva <sup>c</sup>, M. Kostadinova <sup>c</sup>, Ll. Casas <sup>d</sup>, and L. J. Pesonen <sup>a</sup>

<sup>a</sup> *Dept. of Physical Sciences, Division of Geophysics, University of Helsinki, P.O.Box 64, 00014 Helsinki, Finland.*

<sup>b</sup> *Scripps Institution of Oceanography, University of California at San Diego, 9500 Gilman Drive, La Jolla, CA 92093-0225, USA. Phone: +1 858 822 1560; e-mail: fdonadini@ucsd.edu*

<sup>c</sup> *Geophysical Institute, Bulgarian Academy of Sciences, block 3, Acad. Bonchev str., 1113 Sofia, Bulgaria*

<sup>d</sup> *Dept. Geology, Universitat Autònoma de Barcelona, 08193 Bellaterra (Barcelona), Spain*

**Abstract**

This study investigates archaeological artifacts from five sites in Europe: one from Switzerland (Cheyres - baked clay remains from an Iron Age kiln: 700-530BC); one from Bulgaria (Drustur - Medieval kiln: 1200-1300AD); two from Finland (Busö - Medieval kiln: 1570AD and bricks from Helsinki: 1906AD); and one from Russian Karelia (bricks from Valaam: 1856AD).

The goal of the paper is to determine palaeointensity from the archaeological sites mentioned above, as well as to compare the values obtained in different laboratories.

Palaeointensity experiments were mainly carried out at the Division of Geophysics, University of Helsinki and at the Palaeomagnetic Laboratory of the Geophysical Institute in Sofia. Additionally, microwave palaeointensity determinations on few sister specimens from Helsinki bricks and from Drustur kiln were performed in Liverpool. Large amount of rock-magnetic studies accompanies the work in order to find possible explanations for the acceptance or failure of palaeointensity experiments. The encountered difficulties in obtaining reliable palaeointensity results are discussed and show a still incomplete state of art for determination of this important ancient geomagnetic field characteristic.

The accepted new palaeointensity evaluations for different time and space will partly fill up considerable gaps in European palaeointensity databases. Geophysical inference is demonstrated on the basis of virtual axial dipole moment calculated from the new palaeointensity results and its relationship with the CALS7K.2 model calculation and the observatory measurements for the corresponding territories.

Keywords: Palaeointensity, Archaeointensity, Rock-magnetic study.

## 1. Introduction

The Earth's magnetic field (EMF) varies its intensity and direction during time. Studies aiming to define the EMF characteristics at a particular place and time are of particular interest to understand the present behaviour as well as future changes of our planet. Some authors have pointed out the possibility of an imminent reversal (e.g. Hulot et al., 2002; Constable and Korte, 2006); others see a link between the sudden variation in EMF directions and intensities (so called archaeomagnetic jerks) and climate changes (Gallet et al., 2005). Moreover, the importance of EMF studies in the past time is underlined by the fact that its outcome constitutes the raw material to construct theoretical models (e.g. Korte and Constable, 2005).

The present study concentrates on the determination of the intensity of the geomagnetic field (paleointensity). This is possible because well fired archaeological artifacts have the possibility of acquiring a stable thermoremanent magnetization (TRM), which correlates to the direction and intensity of the EMF during the firing of the artifact. Experimentally, the determination of paleointensity requires a number of conditions that are normally not met (e.g. Tarduno et al., 2006). Amongst different methods, the Thellier technique (Thellier and Thellier, 1959) and its modification after Coe (1967), or Yu et al. (2004), are considered as the most reliable because the experimental setup reproduces the natural cooling conditions of the artifact. If the magnetic carrier of the material consists of single domain (SD) particles, the additivity law at the basis of the Thellier experiment is valid. As the mineralogy of archaeological materials is often more complex, several tests have been developed to detect possible thermo-chemical alteration induced by severe laboratory heating (Coe et al., 1978), and to determine the influence of non-ideal SD magnetic grains (Shcherbakova et al., 2000; Riisager and Riisager, 2001; Krasa et al., 2003). Another technique, consisting of heating the samples using microwaves, has been developed by Walton et al. (1991), and has the advantage of being rapidly executed as well as heating only the magnetic carrier. Hence, the bulk matrix of the sample is left untouched and the

alteration is significantly reduced. At present, it is not well known if the blocking temperature of the natural cooling material correlates with the unblocking temperature induced by microwaves. However, some studies (e.g. Casas et al., 2005) show that there is a good agreement between the Thellier and microwave techniques.

The goal of this paper is to determine palaeointensity obtained from different archaeological artifacts from Bulgaria, Scandinavia and Switzerland and to compare the values obtained in different laboratories. The new palaeointensity evaluations will partly fill up considerable gaps in European databases.

## **2. Materials studied and dating**

This study investigates the baked clay artifacts from five different sites. Their geographical location is shown in Fig. 1.

The Medieval site of Drustur (Bulgaria) is dated on the basis of coins (1080-1085) as *terminus post quem* and the imitation of Constantinople Latin coin (type O) related to 3<sup>rd</sup>, 5<sup>th</sup>/6<sup>th</sup> decades of 13<sup>th</sup> century as *terminus ad quem*. The archaeological evidences, coins and stratigraphy determine the time of building and operation of the oven as middle-late 13<sup>th</sup> century (Angelova and Koleva, 2005). The oven is located at 44.1°N – 27.25°E. Oriented baked clay hand-samples were taken from the tongue-like pedestals structures of oven No 1 used for coarse domestic ware firing.

The site of Cheyres is located in the French part of Switzerland (46.81°N - 6.78°E) – Roche-Burnin, Fribourg. From the kiln structure, several non-oriented pieces of baked clay were studied. The date of the structure as based on the ceramic finds indicates an age 750 to 650 BC. There is a radiocarbon date from Upsalla laboratory: 2530 ± 65 BP which calibrates to 810-410 BC at 2σ and 700-530 BC at 1σ (Hedley, 2006, pers. comm.).

The Scandinavian samples consist of two sets of bricks from Helsinki (Finland, 1906 AD, 60.1°N – 24.9°E), and Valaam (Russian Karelia, stamped bricks, AD 1856, 61.3°N – 30.9°E), as well as an oven located at Busö island (Finland, 59.8°N - 23.6°E) where archaeologists carried out detailed investigations (Haggren and Jansson, 2004). From Busö unearthed baked clay parts of the oven have been studied. The Busö Island was part of the Nyland/Uusimaa region, extending from Turku to Helsinki, and comprising the Finnish archipelago. The whole region was colonized during a time spanning between 6<sup>th</sup> and 16<sup>th</sup> century. In particular, the coastal zones of the region were not populated until 12-13<sup>th</sup> century, according to the traditional archaeological knowledge. The age dating of the oven located at Busö is constrained by the finding of coins (Moneta Nova) which circulated for a short period of time around 1570 AD.

### **3. Experimental methods and techniques used for describing the rock-magnetic properties.**

Magnetic measurements have been carried out at Helsinki (Finland) laboratory using an AGICO spinner magnetometer (JR6a) to measure the remanence and at Sofia (Bulgaria) laboratory using a Molspin magnetometer. To investigate the magnetic stability with time, the viscosity coefficient has been determined by the zero-field storage during 3 weeks (Kovacheva and Jordanova, 2001) for Drustur, Cheyres, Busö, and Helsinki sites. To define the magnetic mineralogy comprising the main remanence carriers high temperature susceptibility curves in conjunction with the composite three-axial isothermal remanent magnetization (3IRM) tests (Lowrie, 1990) were used. The irreversibility of the susceptibility curves during the heating-cooling procedure is also an indication of the possible mineralogical changes in the laboratory treatment. Lowrie-Fuller test (Lowrie and Fuller, 1971) and hysteresis analysis were undertaken for evaluating the prevailing domain type of behaviour. To additionally screen the thermal stability of the mineralogy and possible thermo-chemical changes during the laboratory heating, SIRM tests (Jordanova et al., 1997; Kovacheva and Jordanova, 2001; Jordanova et al., 2003)

were also performed. The advantage of the SIRM experiment is that it measures directly the magnetic remanence, carried solely by ferromagnetic minerals. In this experiment we compare the thermal decay curves of SIRM induced only once before heating with that of stepwise induced SIRM at each thermal step (SIRM left). The latter includes all newly generated magnetic phases with deblocking temperatures higher than the previous temperature step. Thermal decay of SIRM induced only once is calculated as the module of the magnetization from the three-axes laboratory induced IRM thermal decay - Lowrie, 1990 (3IRM experiment) of the sister specimen. The coincidence between the two decay curves evidences thermally stable magnetic mineralogy. In contrast, the high temperature susceptibility curves account for all constituent fractions (ferro-, para- dia-, newly born superparamagnetic grains, etc.). For some pilot specimens from the sites Busö, Valaam, and Helsinki the 3IRM tests were performed in Madrid's palaeomagnetic laboratory as well (McIntosh et al., submitted).

High temperature susceptibility curves were performed using the high temperature attachments to KLY2 (Sofia) and KLY3 (Helsinki) AGICO kappabridges.

The hysteresis analyses were performed in Helsinki laboratory using Micromag VSM (Princeton measurements Co.).

Non-magnetic technique such as Mössbauer analysis was performed on the Helsinki and Drustur bricks, at the Institute of Material Sciences in Barcelona (Spain).

#### **4. Magnetic mineralogy and stability of the studied materials.**

All the obtained results are summarized in Table 1. The different experimental procedures are connected with different sub-samples (specimens) coming from one and the same hand sample.

The specimens show in general low viscosity coefficients (less than 10%) with the exception of some specimens from Busö. The inter-specimens discrepancy from Busö hand samples is quite high thus the choice for the palaeointensity experiment has been made accordingly.



The median destructive field (MDF) varies between 15 and 41 mT (Drustur), 18 and 24 mT (Cheyres), 10 and 20 mT (Busö), and about 30 mT and higher (Helsinki and Valaam bricks). Often specimens from Busö, Valaam and Helsinki bricks are characterized by so hard components that their MDF should be reached after AF treatment at 100 mT.

The results of Lowrie-Fuller test (L-F test in Table 1) are given by the parameter

$$\frac{MDF_{NRM} - MDF_{IRM}}{MDF_{NRM}} \quad (\text{Dunlop, 1983})$$

calculated in order to distinguish between single domain (SD), bimodal (BM), multidomain (MD) and mixed like behaviors. Bimodal behavior occurs often in our materials expressing the concurrent presence of fine grains carriers and coarser grains, this is the typical behavior for the non pre-selected clay used in kiln plasters (for example Cheyres and Busö). The clay used to fabricate the bricks from Valaam and Helsinki has been obviously heated to high temperature and these specimens have shown the highest coercivities (Table 1). The evident presence of high coercivity carriers violates the basic conditions of the Lowrie-Fuller test. These results are marked as “high coercivity” in Table 1.

According to the unblocking temperatures of the remanence during the thermal demagnetization of 3IRM test, and taking into account the Curie temperatures revealed by the high temperature susceptibility behavior (HTK) we can conclude that the magnetic carriers for the several studied sites are very variable. In general the magnetically soft minerals prevail (the soft component deblocking – Table 1) in samples from Drustur, Cheyres and BR06 (Helsinki). All samples from Valaam, two samples from Helsinki (HEL1 and HEL2), as well as some from Busö have a substantial - and in some case the maximal relative contribution of hard magnetic minerals. Examples of the 3IRM behavior are shown in Fig. 2. Evidently, hard components detected during 3IRM tests and unblocking at temperatures around and higher than 600°C (Fig. 2b, d, f, g) can be associated with the presence of hematite or its substituted forms. Similarly to a study performed in Madrid (McIntosh et al., submitted), we often identify in these collections a hard

component associated to low unblocking temperature as between 200 and 300°C (Fig. 2b, c, d, f, g).

Curie temperatures were determined according to the second derivative analysis of high temperature behavior of the magnetic susceptibility (Fig. 3), and are shown by the associated minerals in Table 1 (column 8). The main carrier appears to be magnetite (M) or titanomagnetites (TM). In most cases the presence of other minerals like maghemite (MH) and hematite (H) can also be detected.

High temperature susceptibility curves (Fig. 3) reveal different degrees of mineralogical changes by heating. This concerns especially the collection of the site Busö (Table 1 and Fig. 3c). However, the companion experiment (SIRM test) monitoring thermo-chemical changes (Fig. 4) suggests stable mineralogy of the remanence carriers in most of the studied specimens. In Fig. 4 the thermal demagnetization of successively induced SIRM (2T) at each heating step (SIRM left – full diamonds) monitors the newly born magnetic phases with Curie temperatures higher than the previous heating step. This curve is compared with the module of thermal demagnetization of the composite IRM induced only once before the heating (3IRM test) performed on a sister specimen and reflecting the initial mineralogy (3IRM – open squares). When these two curves coincide or are very close it is said that the SIRM test is positive (Fig. 4a, c, e, f) whereas it is negative when they differ substantially (Fig. 4b, d) confirming the thermo-chemical change of the mineralogy - see also Table 1. In case of negative SIRM test the material is considered not very favorable for palaeointensity determination. However, sister specimens can sometimes show different behaviour (e.g. no alteration, positive SIRM), probably due to inhomogeneous heating in the antiquity or inhomogeneities of the material studied.

Hysteresis loops (Fig. 5 and Table 1) reveal often the occurrence of wasp-waisted forms (Fig. 5c, d, e), indicating the coexistence of soft and hard magnetic phases (Roberts et al., 1995). This observation is in agreement with the experimental procedures described previously (Table 1 –

3IRM test and HTK, and Fig. 2 and 3). The strongest effect is observed in the brick samples from Valaam and Helsinki, having in general higher coercivity. Samples from Busö show wasp-waisted loops connected with low and medium coercivities, again in both cases the coexistence of two fractions is evident also from the other measurements. In order to verify the possible influence of the superparamagnetic contribution (Dearing et al., 1996) the frequency dependence of susceptibility ( $X_{fd}$ ) has been measured for some pilot specimens (last column of Table 1), however a systematic relationship with the shape of the hysteresis loops could not be found. Therefore, it appears that in our collection the presence of phases with contrasting coercivity has higher effect on the loop's shape. In general the wasp-waisted loops correlate with the presence of hematite identified by its Curie temperature.

A Day plot for titanomagnetites (Day et al., 1977), using the re-appraisal after Dunlop (2002) is shown in Fig. 6. The results of the main group of studied specimens concentrate in the envelope between the calculated mixture of SD-MD particles and the calculated mixture of SD-SP particles. Some of the results even approach well the space of SD-like behavior. Very well grouped and placed in the PSD region of behavior are the specimens from Cheyres. The results from the site Busö show the highest scatter on the Day diagram, in agreement with the loop shape consistent with the variable coercivity values presented in Table 1. Practically we have no specimens showing  $M_{rs}/M_s$  ratios lower than 0.1. We can not consider specimens having  $H_{cr}/H_c$  values above 5 to be inadequate for palaeointensity determinations mainly because they cannot be determined as dominated by MD carriers. The second reason is that these high values of coercivity ratio can be due to the high  $H_{cr}$  determined mainly by the hard phase, when  $H_c$  is biased towards the co-existing soft phase (Dunlop, 2002). Thus, the distribution of Busö's samples to the right of the PSD region and far away of SD-MD mixing curve suggests the presence of two coercivity phases rather than the large quantity of MD grains. The most clustered data showing favorable hysteresis properties for palaeointensity determinations are

those from the Helsinki bricks. The results of specimens from Drustur lie on the upper part of the PSD space (with two outliers), in accordance with the highest  $X_{fd}$  values (Table 1). We observe that our entire dataset is well displaced along the calculated line of SD-SP mixture, when compared with hysteresis results for similar archaeological baked clays given in Dunlop (2002). One non-magnetic approach (Mössbauer method) has been applied to sample HEL2 (Helsinki) and sample 2403a, and 2338 (Drustur). All spectra show two contributions of  $Fe^{3+}$ : a paramagnetic doublet (that could include a superparamagnetic contributor) and a magnetic sextet with hyperfine field values assignable to hematite confirming previously performed rock-magnetic studies (Table 1). Fig. 7 shows the characteristic pattern for sample HEL2 and 2403a.

## 5. Palaeointensity measurements and results

At Helsinki, the Coe variant (Coe, 1967) of the Thellier method was used to determine the palaeointensity. The samples were cut in standard sized cylinders or cubes, and heated with a Schoenstedt TD1 oven.

In Sofia the samples were cut in standard cubes ( $V=8\text{ cm}^3$ ) and they were heated using a MMTD oven applying the Coe version of palaeointensity experiment, and the magnetization was measured using the Molspin magnetometer. Four specimens from Drustur were studied using the classical Thellier method (Thellier and Thellier, 1959), and the magnetization was measured in this case by the computerized astatic magnetometer with an optical feedback system (Boroc Geomagnetic Laboratory, Russia). These four specimens were allowed to cool slower in the natural Earth's magnetic field ( $38.11\text{ }\mu\text{T}$ ) at the Vitosha mountain laboratory.

At Liverpool, mini-specimen ( $V\cong 1\text{ cm}^3$ ) were prepared from the Helsinki bricks and from the Drustur kiln, and heated in a microwave oven. The magnetization was measured using a built-in SQUID magnetometer inside the Microwave system.

The analysis is performed using the software developed by Leonhardt et al. (2004). Accepted paleointensity value need to fulfill the following criteria: (i) the intensity is determined only in the part of the line where the characteristic remanent magnetization (ChRM) can be observed, (ii) the limit for pTRM checks is chosen as 8% and for pTRM-tail checks as 10%, (iii) 'f' factor preferentially being higher than 0.4 and (iv) at least 6 successive points must be taken into account in the calculation of the slope.

In total, 34 specimens were measured in Sofia, 35 in Helsinki, and 14 in Liverpool. Some examples of Thellier experimental results are shown in Figures 8 and 9. The obtained results are reported in Table 2. All the accepted palaeointensity determinations are included, also evidencing the laboratory where the experiment has been performed. The weighted averages have been calculated using the variance of experimental points in the chosen temperature interval (Kovacheva and Kanarchev, 1986) as a weighting factor (w. mean s) and using the value "w" (w. mean w) as calculated by Thellier tool (Leonhardt et al., 2004). It is evident that these two manners of weighting give very consistent results (Table 2).

According to the 3-sigma rule (Cramer, 1946), paleointensity results that differ from the site mean paleointensity value more than 3 times the standard error are considered as outliers. These values are marked with \*\* in Table 2. The specimens marked with one asterisk are those studied using the classical Thellier method and slowly cooling.

In Helsinki, most specimens from Helsinki and Valaam bricks were measured so that the  $B_{lab}$  field was parallel to the NRM in order to minimize the effects of fabric anisotropy (e.g. Gallet and Le Goff, 2006). In case the specimen's NRM was not aligned with  $B_{lab}$  the tensor of anisotropy of susceptibility (AMS) was used to correct the palaeointensities estimates using the method after Veitch et al. (1984). Even if the effective anisotropy correction should be made using the tensor of anisotropy of remanence (e.g. Chauvin et al., 2000; Hus et al., 2003), we notice that there is a good agreement between paleointensity values where AMS correction was

performed and values obtained by aligning the laboratory field with the NRM. This observation is reflected in Table 2, column 14 and 15, where it can be noticed that these corrections are in general not significant and vary between 1 and 8%.

There is a different angular deviation between the NRM and the direction of the applied laboratory field for the cubes measured in Sofia. We performed the Anisotropy of Anhysteretic Remanent Magnetization (AARM) correction after Thellier experiment on 12 specimens not showing mineralogical alteration as based on the pTRM checks and over one specimen (BU3-2) which obviously had changed its mineralogy during the Thellier experiment (Table 2). Following the results of Hus et al. (2003) we have chosen a window of 0-30mT for applying the ARM for the samples with soft carriers prevailing and full ARM for hard ones. The palaeointensity values corrected for AARM are given in the 4<sup>th</sup> and 5<sup>th</sup> columns of Table 2. Six of the 12 measured AARM give no correction. Another 5 specimens show corrections varying between  $\pm 1\%$  and  $\pm 5\%$ , with one exception (specimen HEL2-2c) giving 11% correction. The specimen with the altered mineralogy (BU3-2) has shown the highest anisotropy correction (-18%), but in fact this correction is not associated with the magnetic carriers giving the palaeointensity evaluation. It appears that the AARM correction is not significant and hence the final average is calculated using the uncorrected values. Gomez-Paccard et al. (2005) made a similar observation in a recent paper: the TRM anisotropy correction was not significant in the determination of the mean palaeointensity per site, and it is in agreement with the detailed study on the subject by Kovacheva et al. (2007, in preparation).

The bricks from Helsinki, Finland, were measured in 3 different laboratories: using the Coe's version of the Thellier method at Helsinki and Sofia and using the microwave technique (Walton, 1991) at Liverpool. In most cases the Helsinki bricks show optimal Arai diagrams during the Thellier experiment, the samples show a unique direction and their mineralogy is stable over the whole palaeointensity experiment. In general the intensities obtained in Sofia

show lower palaeointensity values compared to Helsinki or Liverpool laboratories. The latter two laboratories show a very good agreement (Table 2, Fig. 8). The results of palaeointensity experiments are given by their Arai plots (Arai, 1963). The microwave measurements point out again the presence of a high coercivity phase, as shown by the previous rock-magnetic studies (Fig. 2 and Table 1). The samples could not be completely demagnetized at maximum microwave power, and the 'f' factor ranges in general between 0.33 and 0.52. Additionally, we notice that the standard deviation associated to the single measurements is relatively high (notably for specimens given in italic in Table 2 – 21<sup>st</sup>, 22<sup>d</sup>, 23<sup>d</sup> columns). A mean value using only data with standard deviation of the slope lower than 5% (4 specimens) give a well constrained intensity value of 49.92  $\mu\text{T}$ . It appears that the microwave technique here encounters more difficulties compared to the Thellier determinations because the samples could not be completely demagnetized.

The examples of Arai plots from sites Valaam, Busö and Drustur are shown in Fig. 9.

Valaam samples also show a very good agreement (mean paleointensity: 45.43  $\mu\text{T}$  at Helsinki and 42.16  $\mu\text{T}$  at Sofia). The samples show a unique line between 0 and 500 degrees, and their 'f' factor is often close to 1 (Table 2).

Busö site shows good agreement between the two laboratories (mean paleointensity: 63.68  $\mu\text{T}$  at Sofia and 62.79  $\mu\text{T}$  at Helsinki). Only two specimens (namely BU02-7 and BU11-2) show a value that is conspicuously higher (or lower) compared to the mean and are treated as outliers (marked with \*\* in Table 2). Interestingly, the sister specimens BU11-1 and BU11-2 both gave acceptable results according to criteria, however one of them appears as outlier (Table 2 and Table 3). This can be explained by the above mentioned diversity during the viscosity test when a drastic discrepancy in the viscosity coefficient even intra sub-samples confirms the great non-homogeneity of heating during the antiquity. On the other hand the ChRM is often isolated after 200°C step in the palaeointensity experiment. As a difference from the experimental results of

Helsinki and Valaam bricks described above, the Arai diagrams and Zijderveld plots for most of the specimens from this site show a strong deviation in the lower temperature spectra. Examples are given in Fig. 10.

The site of Drustur, Bulgaria, shows a greater difference between the average results obtained in the Sofia laboratory ( $57.31\mu\text{T}$ ) and the Helsinki laboratory ( $68.2\mu\text{T}$ ). The standard deviations for individual experiments obtained in Helsinki are in general higher than those in Sofia. Of all 17 specimens measured in Sofia and in Helsinki, only the results of 2 specimens were rejected on the basis of the criteria set above, when 4 cases with “F” up to 4% less than stated 0.40 are taken into consideration. The temperature range used for the analyzed samples is similar in both laboratories. There is no evidence of concave Arai diagrams (e.g. Coe et al., 1978), which would lead to biased intensity results. A slight decrease of intensity (3.6%), associated with a small improvement of the standard deviation of the results can be observed when applying the correction for AMS (14<sup>th</sup>, 15<sup>th</sup> columns in Table 2).

Three specimens were measured using the microwave technique at the Liverpool laboratory. Again, we face the problem that the specimens could not be demagnetized at maximum microwave power. It should be immediately mentioned that sample 2391 shows the highest coercivity (Table 1). Additionally, the measurements show a very large standard deviation, hence no average was calculated from those measurements. This obviously again reflects the presence of a hard phase as shown in Fig. 2c and 2d).

Amongst all sites mentioned so far, Cheyres is the one that shows the highest inconsistency between the palaeointensity results of samples measured within each laboratory. The reliable paleointensity values (according to the acceptance criteria) cover a paleointensity range between 20 and  $110\mu\text{T}$ . About half of the results were rejected (e.g. Table 3). Fig.11 depicts two examples of contrasting palaeointensity values when for the lower value the presence of a second component is evident. In general both Arai diagram and Zijderveld plot are ideal, and agree with



the good rock magnetic properties established previously, for example the positive SIRM test revealing minimal physico-chemical alteration. However, a look at the variation of the susceptibility during the paleointensity experiments indicates that changes occur already at low temperatures (200° C).

Cheyres site, dated by  $^{14}\text{C}$  in Upsalla (2530±65BP) as Hallstatt in Switzerland (700-530BC), corresponds to Bulgarian Thracian time. For this period of time the palaeointensity in Bulgaria varies between 70 and 80  $\mu\text{T}$  (Kovacheva, 1997) - quite a high value when the geographical latitudes are lower than that of Cheyres. Thus, for the site of Cheyres, the expected value should be around 80  $\mu\text{T}$  or even higher. A detailed examination of the experimental results leads to only five results close to the expected values from 15 specimens studied and 8 passing the stated criteria. Hence, no conclusive result can be drawn from this site.

The overall inspection of the obtained results (Table 2) reveals that in general all sites show slightly higher intensities and higher standard deviations when the measurement is performed in Helsinki. This deviation is in the order of 5-10%, with exception of Drustur for which the difference between the average values obtained in the two laboratories is 16%. The only major difference between the two laboratories is the type of laboratory furnace used. In Helsinki it has been necessary to move the samples from the heating to the cooling chamber, whereas in Sofia the samples have not been moved during the entire experiment. Hence, in Helsinki there is a risk that the specimens can be in some way disturbed during this movement. The laboratory field is switched on only after the sample has been moved to the cooling chamber, and this might lead to irregular difference between the temperature of the step and the upper limit of the pTRM induced. Such an effect leads logically to the artificial decrease of laboratory pTRMs which can explain the systematic difference in the obtained palaeointensity values and the higher standard deviations of the mean compared to those from Sofia (MMTD furnace).

## 6. Discussion

The palaeointensity determinations presented here and performed using different kind of materials at three different laboratories employing different techniques reveal the extreme difficulties often encountered in archaeomagnetism for obtaining reliable palaeointensity values. The acceptance criteria (based on the limits of pTRM and pTRM-tail checks, as well as the fraction of the NRM used) are independent from the precision and accuracy of the mean intensity value. There is a link between the acceptance criteria and the success of a palaeointensity experiment, which mainly depends on the magnetic properties of the materials and on the homogeneous heating in the antiquity. The latter, if not fulfilled, leads to a chemical equilibrium during the laboratory heating rather than during the antiquity. In Table 3 we show the samples rejected on the basis of the acceptance criteria, indicating the pTRM check and pTRM tail check, or the case of outliers, and the rock magnetic evidence for the failure.

We notice that most of the rejected results are accompanied by the negative SIRM test evidencing the neo-formation of magnetic mineral (thermo-chemical alterations) during the laboratory heating (Jordanova et al., 2003) or by the presence of the ‘High Coercivity, Stable, Low Temperature deblocking phase’ (HCSLT, see the deblocking temperatures of the hard component in Tables 1 and 3). This latter phase appears to be thermally stable (Fig. 13) and is in agreement with observations after McIntosh et al. (2007, submitted). The question raising is why the presence of this phase had not influenced in a similar way the palaeointensity experiment (e.g. Figs. 8, 9 and 10). Considering the 5 sites we notice that the phase is less pronounced in the case of Cheyres (Fig. 12) and in some cases not encountered in the samples from Drustur (Table 1). For samples from Helsinki, Valaam and Busö the HCSLT strongly prevails (Fig. 2b, f and g). The coercivity values as well as the wasp-waisted hysteresis loops are also affected by its contribution (Table 1). We should underline that the hardness of the Helsinki and Valaam bricks is influenced by the additional presence of hematite (Table 1), but the latter cannot interfere with

the success of the palaeointensity experiment. Hence the HCSLT phase alone appears not to be responsible for the acceptance or rejection of our paleointensity measurements.

Compared to the Helsinki and Valaam collections the Busö site gave less satisfactory results. In this case the problem can be associated with a multi-component TRM formed during the ancient firing (Fig. 10). The same behavior was also noticed for samples from Cheyres (Fig.12a). We observe that beside the presence of HCSLT phase, the remanence carried by the Helsinki and Valaam bricks is formed by one magnetic component and is stable over the heating process. When the rejected results are not linked with the thermo-chemical changes (negative SIRM) we have observed at least 2 distinct magnetic components.

If we consider the results of rock-magnetic tests, we should expect good palaeointensity determinations for samples from Cheyres. Nevertheless the susceptibility behaviour during the stepwise laboratory heating evidences often the progressive change in magnetic capacity after 300°C, both for samples consolidated with the water glass and for those without consolidation (Kostadinova et al., 2004). The latter is evidenced by the susceptibility monitoring during the Thellier experiment, and confirms that these changes are associated with non sufficient burning in the antiquity. Obviously in this collection we encounter once more the effect of inhomogeneous heating in the antiquity already noticed when samples were gathered (Ian Hedley – personal communication). We do not find the answer to the fact that the sub-samples (specimens) used for the rock-magnetic experiments C21b, d show no thermo-chemical changes (SIRM positive, Table 1) when C21a used for palaeointensity determination has a rejected result because of bad pTRM tests (Table 3). Thus we cannot give any reliable results for the palaeointensity from this site.

Up to here we have discussed the palaeointensity results in connection with the samples' magnetic properties. However the success of palaeointensity experiment depends a lot on the reciprocity (or its lack) between the pTRMs blocking and unblocking temperatures (Shcherbakov

et al., 2001). Unfortunately the tail checks performed in our study (Riisager and Riisager, 2001) can be detected reliably only when the applied laboratory field is parallel to the carried NRM and it is higher to the ancient palaeointensity (Yu et al., 2004). It has been mentioned above that during the Coe's method application (in Sofia and Helsinki) the laboratory field had generally a random orientation in respect to the NRM (41 cases of 48 accepted results). Thus we hope that in this way the strong dependence of the pTRM tail on the mutual orientation is also randomized. The angular independence of the tail is valid when the classical Thellier method is used as for the three samples of Drustur mentioned with asterisk in Table 2.

The microwave technique applied to the sites of Helsinki and Drustur reveals that the samples are often hard to demagnetize. This can result as a combination of the presence of hard magnetic phases in the samples and technical problems with the microwave equipment.

## **7. Geophysical application**

Table 4 summarizes the mean intensity results in terms of measured ancient field  $B_a$  ( $\mu\text{T}$ ) and VADM ( $10^{22} \text{ Am}^2$ ).

We can plot the mean results obtained from the different sites using the master curves as drawn from the GEOMAGIA50 database (Donadini et al., 2006). The three Scandinavian sites are shown in Fig. 14a, and are compared with the whole Scandinavian dataset. Additionally, the direct observatory data from Nurmijärvi ( $60.5^\circ\text{N}$ ,  $24.6^\circ\text{E}$ ) are shown as a black line, starting 1800 AD to present (Nevanlinna, pers. comm.). We observe that the result from Busö correlates well with the rest of the dataset as well as with the CALS7K.2 model (asterisks) of Korte and Constable (2005). The Valaam and Helsinki bricks show a good correlation with the rest of the dataset; however, the values are slightly lower compared to the direct observations from Nurmijärvi observatory.

The mean result for the Bulgarian site of Drustur (Figure 14b, black diamond) is plotted and compared with the Bulgarian dataset (open circles). It appears that this result placed according to the archaeological assumption for the last usage shows slightly higher values compared to the Bulgarian dataset and to the CALS7K model (asterisks) of Korte and Constable (2005). The palaeointensity result obtained here in combination with the directional studies performed in the Sofia laboratory will further elucidate this non-agreement.

## **8. Conclusions.**

The present study shows that the agreement between the different laboratories is in general good, the differences between the laboratories being in most of the cases less than 10%. The values obtained in Helsinki are systematically shifted towards higher intensities, but in general the difference is not significant. The reason can be searched in an inadequate furnace used during this experiment.

Four new determinations of the palaeointensity have been obtained for Helsinki, Valaam, Busö, and Drustur. The Swiss site located at Cheyres shows a very low precision of the reliable results, and it is hence impossible to draw any conclusion.

The paper shows that the detailed knowledge of magnetic properties of studied materials helps substantially to understand the samples' behaviour during the palaeointensity experiment and also the choice of the specimens to be used for that. The efficiency of the thermal demagnetization of 3-axes laboratory induced isothermal remanence (Lowrie, 1990) and the thermo-chemical stability of the mineralogy (SIRM test, Jordanova et al., 1997) is acknowledged.

The inability to completely demagnetize the samples when using the microwave technique could be explained by the important fractions of magnetically hard phases, in contrast with the low-coercivity ones met in the cases studied by Böhnell et al. (2003) and Casas et al. (2005). The

present trend in the development of the Microwave technique is to increase the maximum applied power, this could solve the problems that have been encountered here using this technique.

The inference of the newly diagnosed (McIntosh et al., submitted) magnetically hard phase in the baked clay materials with the palaeointensity evaluation merits further and deeper investigation.

Several difficulties arise in the palaeointensity determination from the studied collections and make us underline the existing limits in our knowledge to evaluate this substantial characteristic of the past geomagnetic field. Nevertheless, our experiments suggest that the effect of remanence anisotropy on the palaeointensity results obtained from baked clays and bricks is not significant.

To conclude, the database of geomagnetic field intensities has been refined with four new results, which agree with other published data. Two Scandinavian sites: Helsinki (1906 AD,  $VADM = 6.70 \pm 0.13 \cdot 10^{22} \text{Am}^2$ ), and Busö (1570 AD,  $VADM = 8.90 \pm 0.11 \cdot 10^{22} \text{Am}^2$ ) are dated archaeologically or historically. The other Scandinavian site of Valaam (1856 AD,  $VADM = 6.03 \pm 0.19 \cdot 10^{22} \text{Am}^2$ ) is dated by means of stamped bricks, and hence it possesses a very well constrained age.

The Bulgarian site of Drustur (archaeologically related to 1250 AD;  $VADM = 9.70 \pm 0.42 \cdot 10^{22} \text{Am}^2$ ) shows slightly higher values compared to other published data.

### **Acknowledgements**

The study has been carried out during the bilateral exchange program of the Academy of Finland and the Bulgarian Academy of Sciences, and also partially supported by the AARCH EU contract No HPRN-CT-2002-00219 (Archaeomagnetic Applications for the Rescue of Cultural Heritage). We thank Ian Hedley for giving us the Swiss baked clays from Cheyres and Martí Gich for helping us with the Mössbauer measurements. Thanks are due to N. Jordanova who participated in the sampling of Drustur.

## References

- Angelova, St. and Koleva, R., 2005. Kilns for firing everyday pottery from Drustur. *Studia Archaeologica Universitatis Serdicensis. Supplement IV*, 10-20. (in Bulgarian).
- Arai, Y., 1963. Secular variation in intensity of the past geomagnetic field. MSc Thesis, University of Tokyo, Tokyo, Japan, 84pp.
- Bohnel, H., Biggin, A.J., Walton, D., Shaw, J. Share, J.A., 2003. Microwave palaeointensities from a recent Mexican lava flow, baked sediments and reheated pottery. *Earth and Planetary Science Letters*, 6751, 1-16.
- Casas, Ll., Shaw, J., Gich, M., Shaw, J.A., 2005. High-quality microwave archaeointensity determination from an early 18th century AD English brick kiln. *Geophysical Journal International*, 161: 653-661.
- Chauvin, A., Garcia, Y., Lanos, Ph. and Laubenheimer, F., 2000. Paleointensity of the geomagnetic field recovered on archaeomagnetic sites from France. *Physics of the Earth and Planetary Interiors*, 120, 111-136.
- Coe, R.S., 1967. The determination of paleo-intensities of the Earth's magnetic field with emphasis on mechanisms which could cause non-ideal behaviour in Thellier's method. *Journal of Geomagnetism and Geoelectricity*, 19, 157-179.
- Coe, R.S., Gromme, C.S., Mankinen, E.A., 1978. Geomagnetic paleointensities from radiocarbon-dated lava flows on Hawaii and the question of the Pacific nondipole low. *Journal of Geophysical Research*, 83, 1740-1756.
- Constable, C., and Korte, M., 2006. Is Earth's magnetic field reversing? *Earth and Planetary Science Letters*, 246 (1-2), 1-16.
- Cramer, H., 1946. *Mathematical methods of statistics*. Stockholm, Publ. Mir, Moscow, 1975 (translation in Russian).
- Day, R., Fuller, M.D., and Schmidt, V.A., 1977. Hysteresis properties of titanomagnetites: grain size and composition dependence. *Physics of the Earth and Planetary Interiors*, 13, 260-266.
- Dearing, J.A., Dann, R.J.L., Hay, K., Lees, J.A., Loveland, P.J., Maher, B.A., O'Grady, K., 1996. Frequency-dependant susceptibility measurements of environmental materials. *Geophysical Journal International*, 124: 228-240.
- Donadini, F., Korhonen, K., Riisager, P., and Pesonen, L.J., 2006. Database for Holocene geomagnetic intensity information. *EOS, Transactions, American Geophysical Union*, 87 (14), 137

- Dunlop, D.J., 1983. Determination of domain structure in igneous rocks by alternating field and other methods. *Earth and Planetary Science Letters*, 63, 353-367.
- Dunlop, D.J., 2002. Theory and application of the Day plot (Mrs/Ms versus Hcr/Hc). 2. Application to data for rocks, sediments and soils. *Journal of Geophysical Research*, 107, NO. B3, 10.1029/2001JB000487.
- Gallet Y., Genevey A., and Fluteau F., 2005. Does Earth's magnetic field secular variation control centennial climate change? *Earth and Planetary Science Letters*, 236, 339-347.
- Gallet, Y., and Le Goff, M., 2006. High-temperature archeointensity measurements from Mesopotamia. *Earth and Planetary Science Letters*, 241, 159–173
- Gomez-Paccard, M., Chauvin, A., Lanos, Ph., Thiriot, J., Jimenez-Castillo, P., 2006. Archaeomagnetic study of seven contemporaneous kilns from Murcia (Spain). *Physics of the Earth and Planetary Interiors*, 157, 16-32.
- Haggren, G., and Jansson, H., 2004. New lights on the colonization of Nyland / Uusimaa. *Ennen ja nyt*, 4.
- Hulot, G., Eymin, C., Langlais, B., Manda, M., and Olsen, N., 2002. Small-scale structure of the geodynamo inferred from the Oersted and Magsat satellite data. *Nature*, 416, 620-623
- Hus, J., Ech-Chakrouni, S., Jordanova, D. and Geeraerts, R., 2003. Archaeomagnetic Investigation of Two Mediaeval Brick Constructions in North Belgium and the Magnetic Anisotropy of Bricks. *Geoarchaeology*, 18, No 2, 225-253.
- Jordanova, N., Petrovsky, E. and Kovacheva, M., 1997. Preliminary rock magnetic study of archeomagnetic samples from Bulgarian prehistoric sites, *Journal of Geomagnetism and Geoelectricity*, 49, 543-566.
- Jordanova, N., Kovacheva, M., Hedley, I. and Kostadinova, M., 2003. On the suitability of baked clays for archaeomagnetic studies as deduced from detailed rock-magnetic studies, *Geophysical Journal International*, 143, 146-158.
- Korte, M. and Constable, C. G., 2005. The geomagnetic dipole moment over the last 7000 years - new results from a global model. *Earth and Planetary Science Letters*, 236, 348-358.
- Kostadinova, M., Jordanova, N., Jordanova, D. and Kovacheva, M. Preliminary study on the effect of water glass impregnation on the rock-magnetic properties of baked clay. *Studia Geophysica Geodetica*, 48 (2004), 637-646.
- Kovacheva, M. and Kanarchev, M., 1986. Revised archeointensity data from Bulgaria. *Journal of Geomagnetism and Geoelectricity*, 38, No 12, 1297-1310.



- Kovacheva, M. Archaeomagnetic database from Bulgaria: the last 8000 years. *Physics of the Earth and Planetary Interiors*, 102, 1997, 145-151.
- Kovacheva, M. and Jordanova, N., 2001. Bulgarian archaeomagnetic studies: a review of methodological progress and applications in archaeology. *Proceed. of Workshop "Archaeometry in archaeology: new trends", Rhodes, 3-6.11.1999*. In: *Journal of Radioanalytical and Nuclear Chemistry*, (guest ed. I. Liritzis), 247 (3), 685-696.
- Kovacheva, M., Chauvin, A., Lanos, Ph., Jordanova, N. and Karloukovski, V. (in preparation) Archaeointensity study of different archaeological structures. Anisotropy effect on the palaeointensity results.
- Krasa, D., Heunemann, C., Leonhardt, R., and Petersen N., 2003. Experimental procedure to detect multidomain remanence during Thellier-Thellier experiments. *Physics and Chemistry of the Earth*, 28, 681-687.
- Leonhardt, R., Heunemann, C. and Krása, D., 2004. Analyzing absolute palaeointensity determinations: Acceptance criteria and the software ThellierTool4.0. *Geochemistry Geophysics Geosystems*, 5(12), doi: 10.1029/2004GC000807.
- Lowrie, W. and Fuller, M., 1971. On the alternating field characteristics of multidomain thermoremanent magnetization in magnetite, *Journal of Geophysical Research*, 76, 6339-6349.
- Lowrie, W., 1990. Identification of ferromagnetic minerals in a rock by coercivity and unblocking temperature properties. *Geophysical Research Letters*, 2, 159-162.
- McIntosh, G., Kovacheva, M., Osete, M.L., Catanzariti, G. and Rakowski, A. (in preparation). High coercivity phases in the materials used in archaeomagnetic studies.
- Riisager, P. and Riisager, J., 2001. Detecting multidomain magnetic grains in Thellier palaeointensity experiments. *Physics of the Earth and Planetary Interiors*, 125, 111-117.
- Roberts, A.P., Cui, Y.L., Verosub, K.L., 1995. Wasp-waisted hysteresis loops: Mineral magnetic characteristics and discrimination of components in mixed magnetic systems. *Journal of Geophysical Research*, 100, 17, 909-17, 924
- Shcherbakova, V., Shcherbakov, V. and Heller, F., 2000. Properties of partial thermoremanent magnetization in pseudosingle domain and multidomain magnetic grains. *Journal of Geophysical Research*, 105, N0 B1, 767-781.
- Shcherbakov, V.P., Shcherbakova, V.V., Vinogradov, Y.K. and Heider, F., 2001. Thermal stability of pTRMs created from different magnetic states. *Physics of the Earth and Planetary Interiors*, 126, 59-73.

- Tarduno, J.A., Cottrell, R.D., and Smirnov, A.V., 2006. The paleomagnetism of single silicate crystals: Recording geomagnetic field strength during mixed polarity intervals, superchrons, and inner core growth. *Reviews of Geophysics*, 44, Art. No. RG1002.
- Thellier, E. and Thellier, O., 1959. Sur l'intensité du champ magnétique terrestre dans le passé historique et géologique. *Annales Géophys.*, 15, 285-376.
- Veitch, R.J., Hedley, I.G. and Wagner, J.-J., 1984. An investigation of the intensity of the geomagnetic field during Roman times using magnetically anisotropic bricks and tiles. *Archives des Sciences Genève*, 37, 359-373.
- Walton, D., 1991. A New Technique for Determining Palaeomagnetic Intensities. *Journal of Geomagnetism and Geoelectricity*, 43, 333-339.
- Yu, Y., Tauxe, L. and Genevey, A., 2004. Toward and optimal geomagnetic field intensity determination technique. *Geochemistry, Geophysics, Geosystems*, vol. 5, No 2. *An Electronic Journal of the Earth Sciences*, Q02H07, doi: 10.1029/2003GC000630.

## TABLE AND FIGURE CAPTIONS

Table 1: Rock magnetic experimental results. Sv represents the viscosity coefficient, MDF the median destructive field. L-F test shows the Lowrie-Fuller test with the values  $\Delta\text{MDF}/\text{MDF}_{\text{NRM}}$ , as determined in Dunlop (1983); 3IRM shows the deblocking temperatures for soft, intermediate (int.), and hard components ('-' appears when the corresponding component has insignificant contribution to the remanence). The mineralogical change is defined on the basis of the reversibility of the heating and cooling curves (Fig. 3) during the high-temperature susceptibility behaviour and the supposed magnetic minerals (TM-titanomagnetites; M-magnetite; H-hematite; MH-maghemite; G-goethite). The SIRM test shows its success or failure (see the text). Hysteresis parameters are represented as  $M_s$  (saturation magnetization),  $M_r$  (remanent magnetization),  $H_c$  (coercive field), and  $H_{cr}$  (coercivity of remanence). The last column consists of the measured susceptibility frequency dependence in percentage.

Table 2. Summary of the palaeointensity results measured in Helsinki, Sofia, and Liverpool. The table shows the temperature interval ( $T_{\min}$  to  $T_{\max}$ ) used to determine the ancient field  $B_a$ , the standard deviation of  $B_a$  ( $\sigma B_a$ ), the quality factor (q), the NRM fraction used (f) and the weighted factor (w) as defined by Coe et al. (1978), using the software after Leonhardt et al. (2004). The intensity values corrected for the AMS ( $B_{a,\text{AMS}}$ ), in case that the specimen's NRM was not oriented along the applied field are given in 14<sup>th</sup> and 15<sup>th</sup> columns, when the evaluated corrected values on the basis of the laboratory induced anhysteretic remanence on the specimens used in the palaeointensity experiment are given in 4<sup>th</sup> and 5<sup>th</sup> columns. Values from the microwave experiment (Liverpool) expressed in italic have a large standard deviation ( $> 5\%$ ) and are not included in the mean. Values marked with \* were obtained using the classic Thellier method (Thellier and Thellier, 1959), whereas values marked with \*\* fail as based on the 3 sigma rule.

Table 3. The list of specimens with rejected palaeointensity results and some peculiarities characterizing each of them. If linearity of the Arai plot was observed, numerical pTRM and tail checks failures [%] are given. Outliers are those specimens that passed the selection criteria, but gave odd paleointensity values. Rock magnetic evidences are taken from Table 1. HCS LT refers to the thermally stable, magnetically hard phase deblocking at low temperature. BM refers to bimodal (Dunlop, 1983) behaviour. SIRM is a positive or negative test, as explained in the text. Sv is the viscosity index.

Table 4. Summary of the mean intensities values  $B_a$  obtained from the different laboratories, and their standard deviation ( $\sigma B_a$ ), calculated as arithmetic (arith.) mean, as weighted mean using the inverse standard deviation (w. mean s), or using the w-factor (w. mean w). The general mean of all accepted individual results is also expressed indistinctly from laboratory as ancient field intensity [ $\mu T$ ], or as a virtual axial dipole moment (VADM) [ $10^{22} \text{ Am}^2$ ].

Figure 1. Site location on the map of Europe: Bulgarian site of Drustur; Scandinavian bricks (Helsinki and Valaam) and oven (Busö); Swiss site of Cheyres.

Figure 2: Examples of 3IRM test: thermal demagnetization of laboratory induced 3-axes isothermal remanence by 2T, 0.46T and 0.23T separating the magnetic carriers to hard (triangle), intermediate (circles) and soft fractions (squares).

Figure 3. High temperature behaviour of the magnetic susceptibility for specimens from Cheyres, Drustur, Busö, Helsinki and Valaam showing various mineralogical stability with heating.

Figure 4. Examples of SIRM test, monitoring chemico-physical changes during laboratory heating for specimens from the five studied sites. Detailed explanations given in the text. Susceptibility (K) is represented as asterisk, SIRM (2T) as a solid triangle, SIRM left as a solid diamond, and 3IRM as a open square.

Figure 5. Examples of hysteresis loops determined on samples from the studied sites.

Figure 6. Hysteresis properties represented as Day plot (Day et al., 1977): samples from Busö (full circles), from Helsinki (open triangles), from Valaam (full diamonds), from Cheyres (open

squares) and from Drustur (crosses). Dashed lines represent the boundaries introduced by Dunlop (2002).

Figure 7. Mössbauer spectra of the samples HEL2 (Helsinki) and 2403a (Drustur).

Figure 8. Example of comparative palaeointensity experiments from the Helsinki brick (1906 AD) performed in Helsinki, Sofia and Liverpool laboratories. Arai diagrams with their pTRM checks.

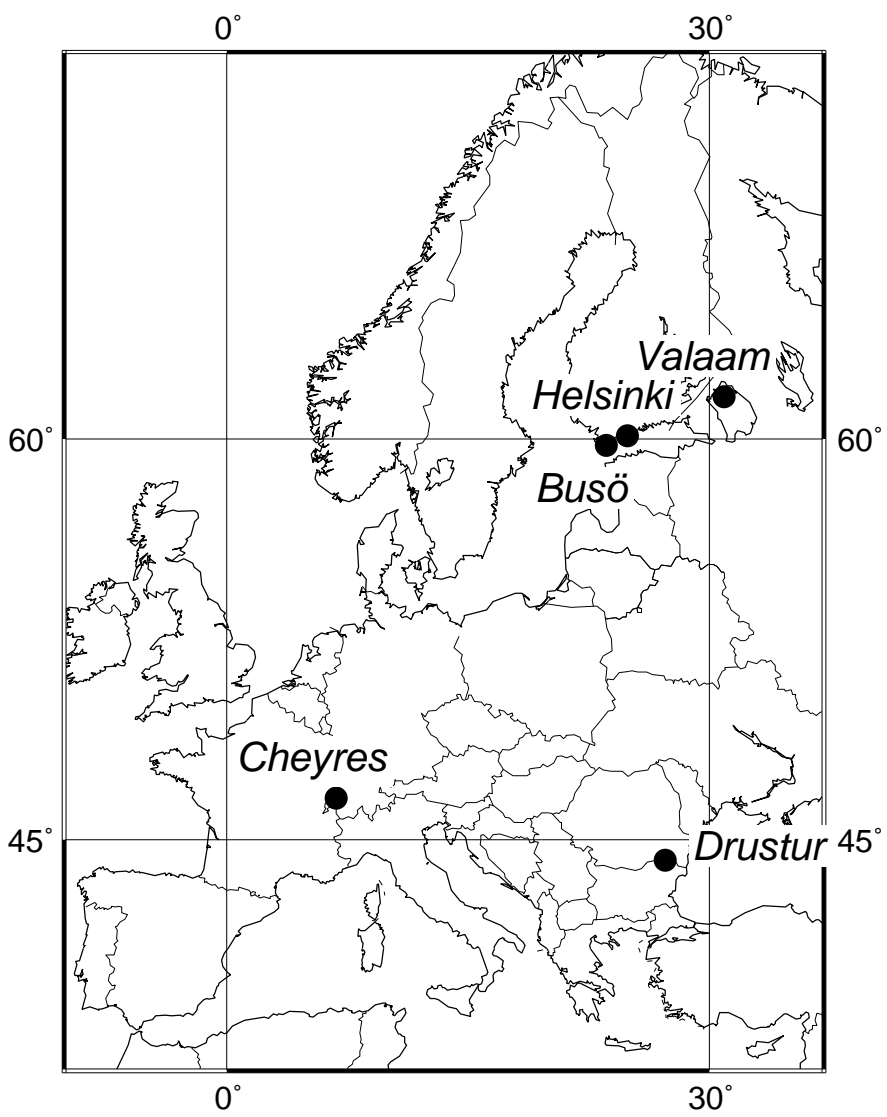
Figure 9. Examples of successful palaeointensity determinations performed in the laboratories of Helsinki and Sofia for the materials from the sites of Valaam (a), Busö (b), and Drustur (c).

Figure 10. The Arai diagram and Zijderveld orthogonal plots for specimens from the site Busö.

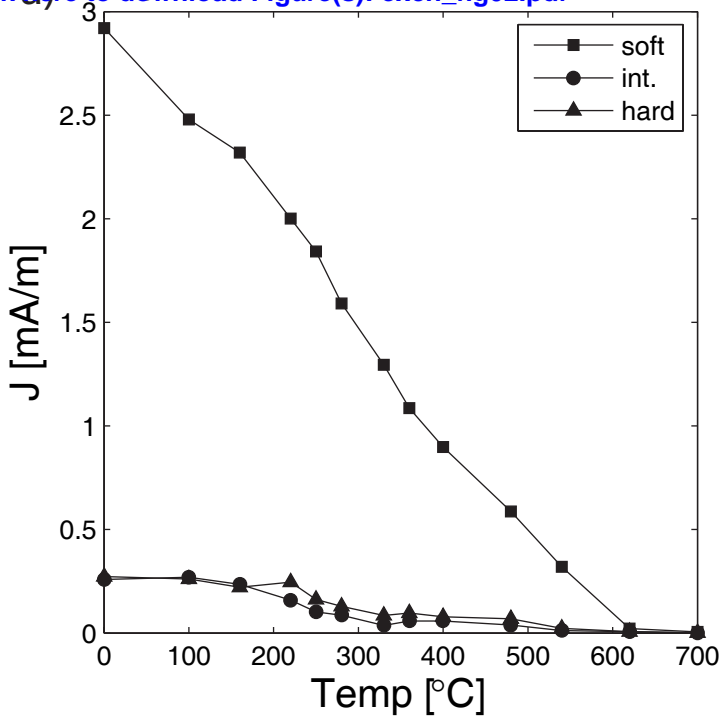
Figure 11. Two contrasting Arai and Zijderveld's orthogonal plots showing a low (a) and a high paleointensity result (b) from the site Cheyres.

Figure 12. Thermal stability of the low-temperature deblocking hard magnetic phase (HCSLT) revealed by the repeated 3 axes IRM (3IRM) experiment over the same specimens.

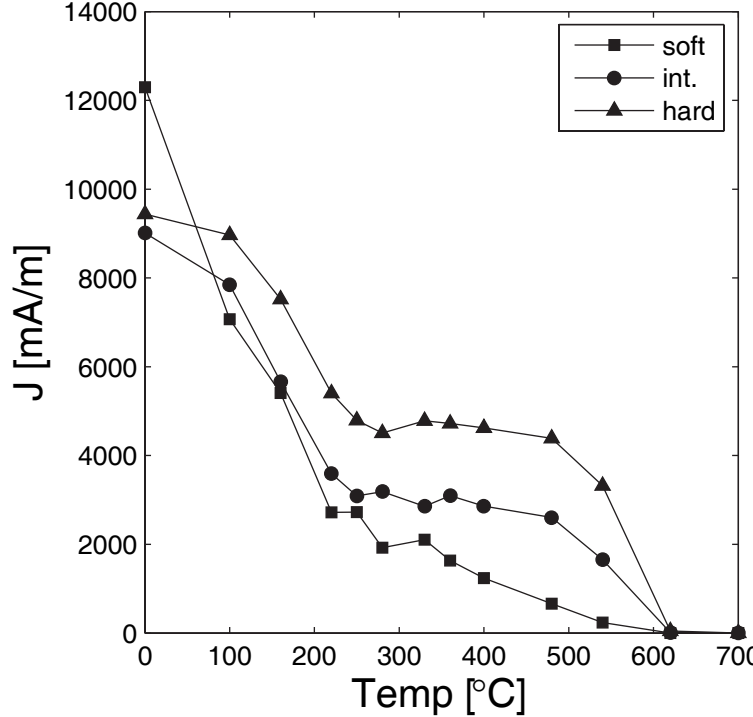
Figure 13. a) VADM for Scandinavia (open circles), and the 3 new results for Busö (1570 AD, closed square), Valaam (1856 AD, closed triangle), and Helsinki (1906 AD, closed diamond). Black line shows the Nurmijärvi direct observations. b) Virtual Axial Dipole Moment (VADM, open circles) of Bulgarian data and the new result from Drustur (closed diamond). The trend line given with asterisks represents the CALS7K.2 model of Korte and Constable (2005).



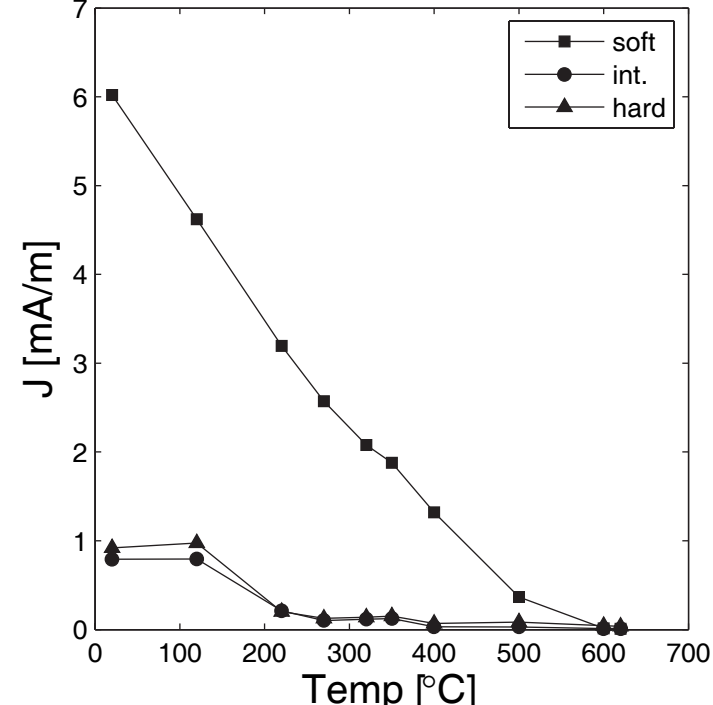
Cheyres - C15d



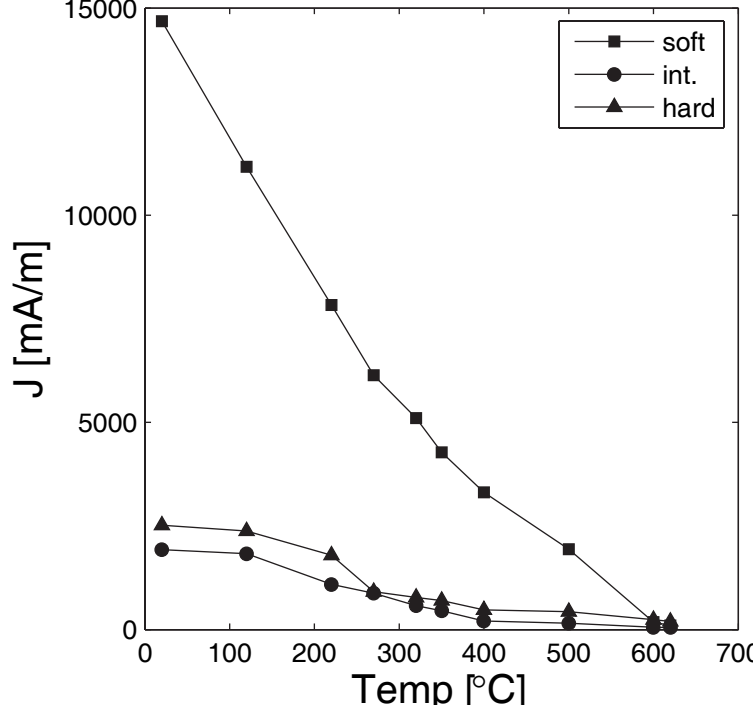
Valaam - VT2-1



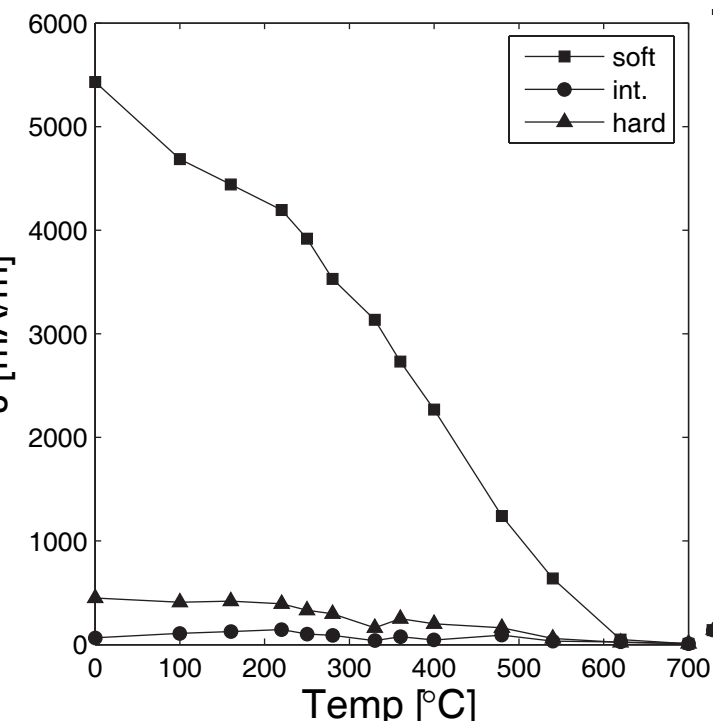
Drustur - 2398a



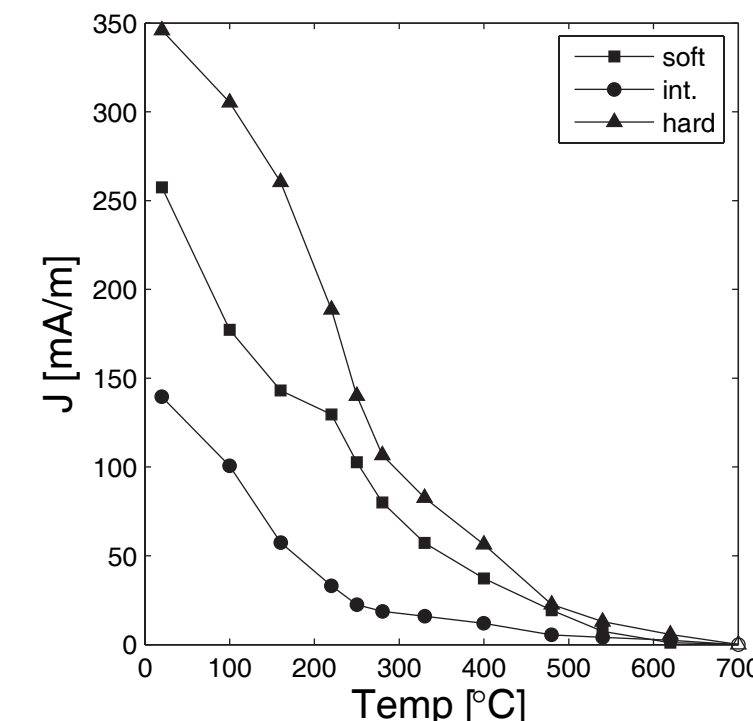
Drustur - 2400b



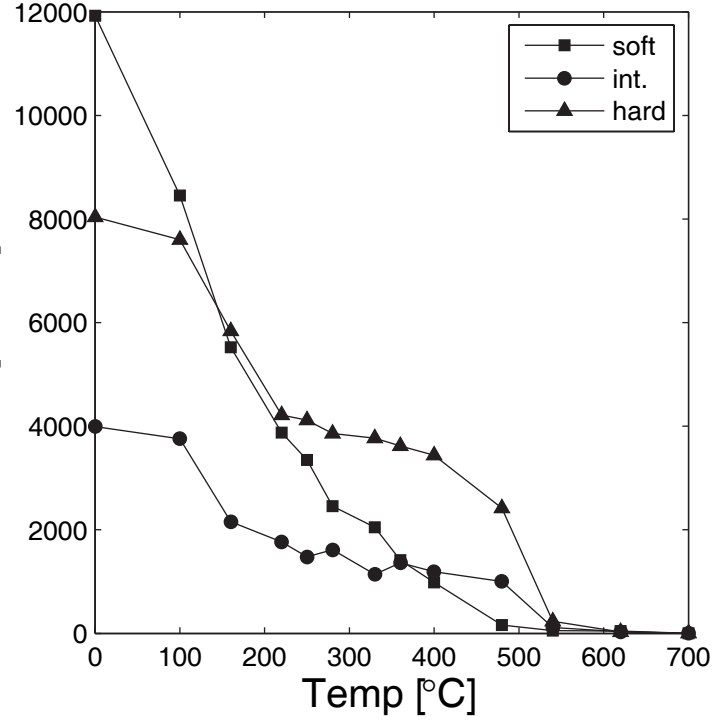
Busö - BU02-3



Busö - BU04-2



Helsinki - HEL2-6f



Helsinki - BR06-2a

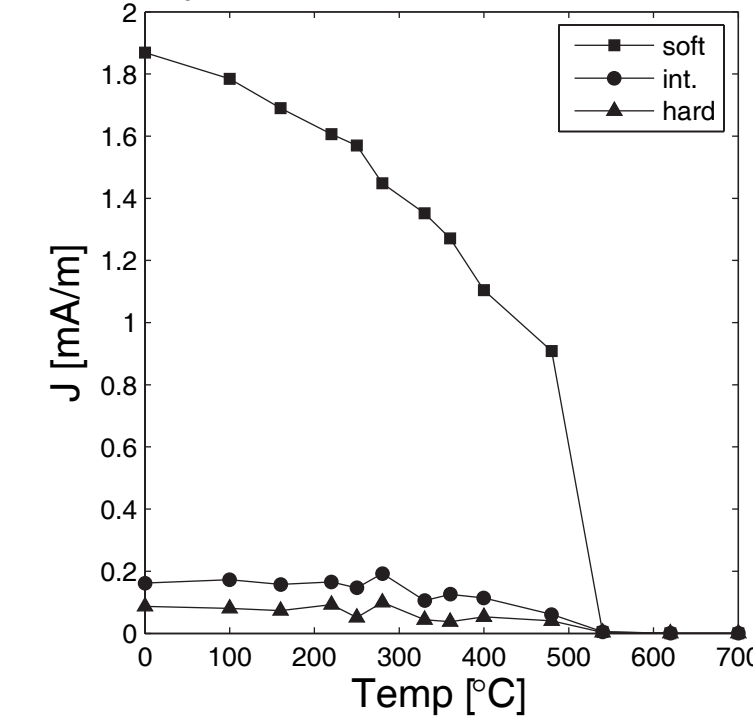
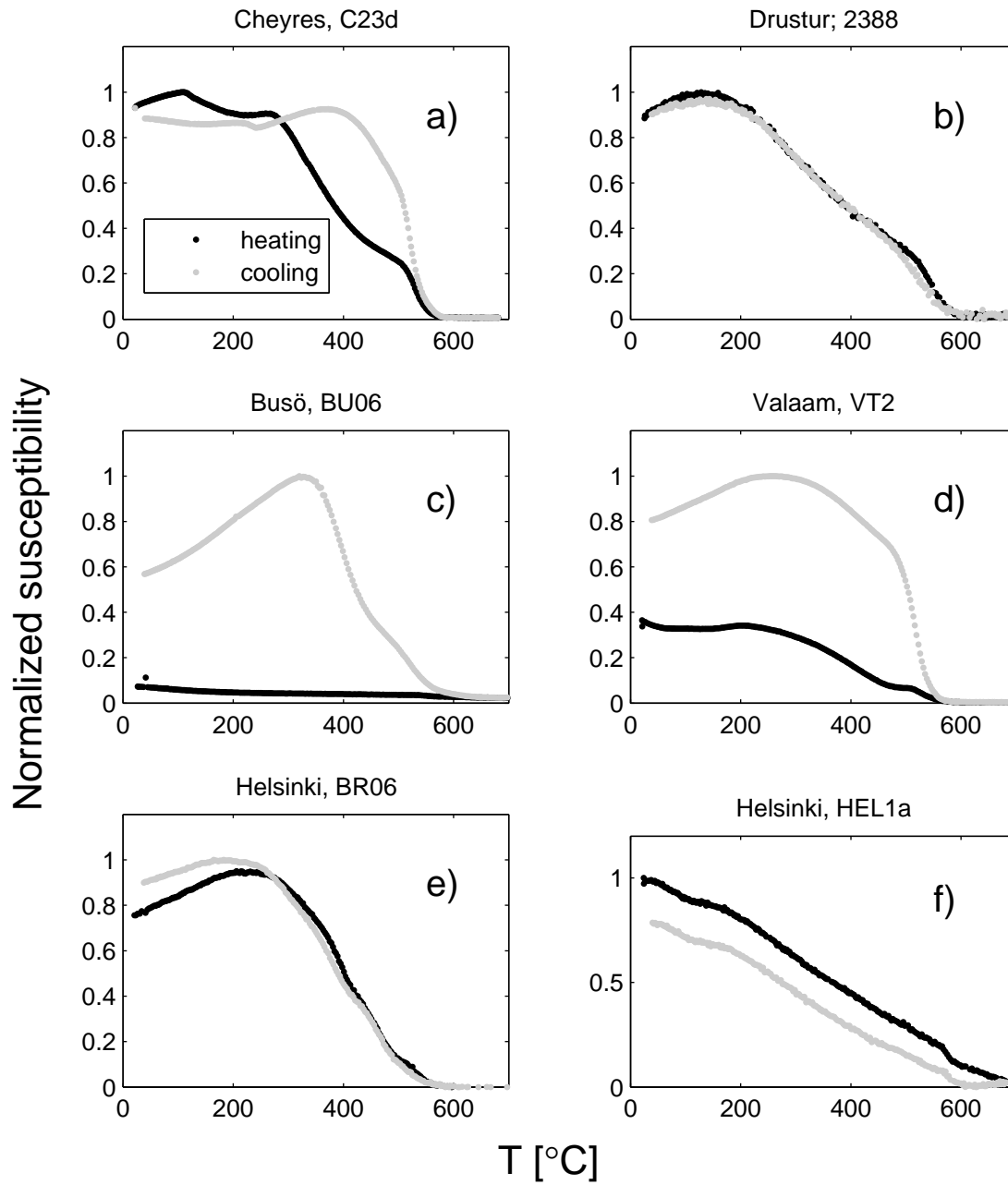
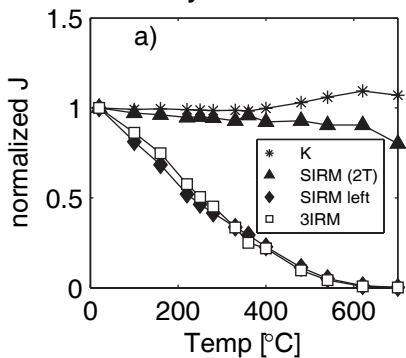
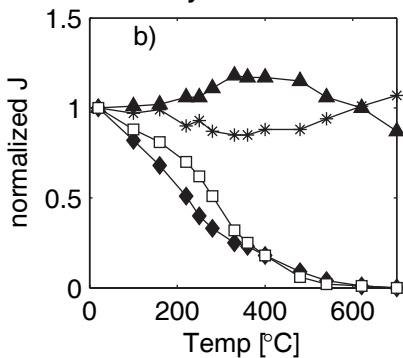
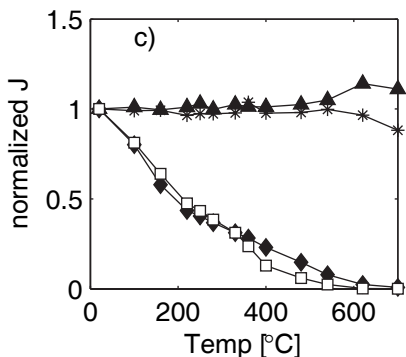
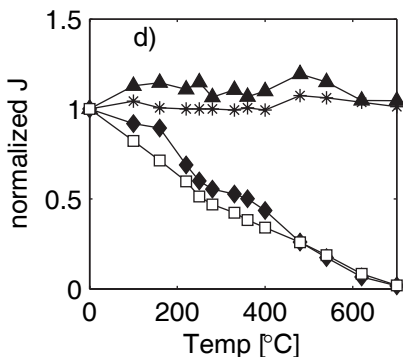
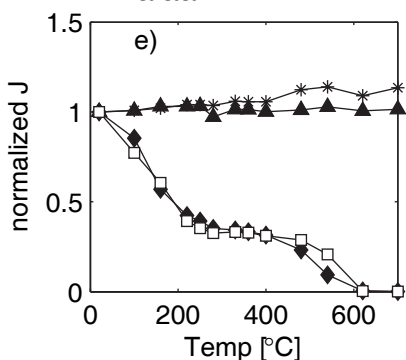
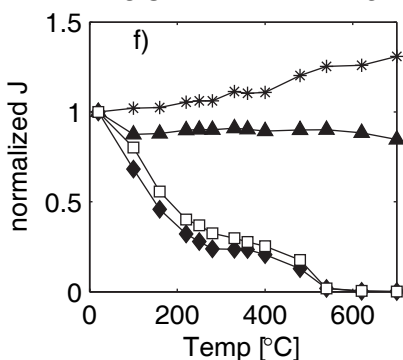


Figure 03

[Click here to download Figure\(s\): exch\\_fig03.pdf](#)





**Figure 04**[Click here to download Figure\(s\): `exch\_fig04.pdf`](#)**Cheyres – C16b****Cheyres – C23c****Drustur – 2403v****Buso – BU05a – 1****Valaam – VT2 – 2****Helsinki – HEL2 – 6f**

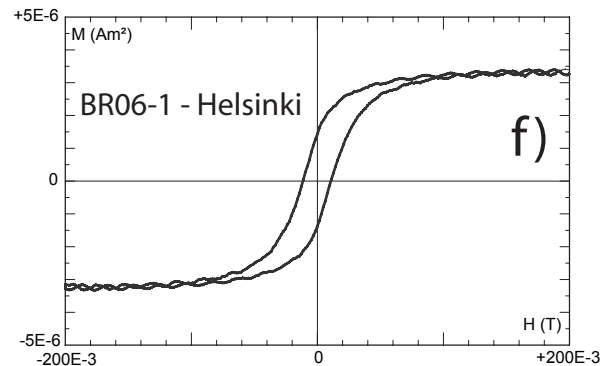
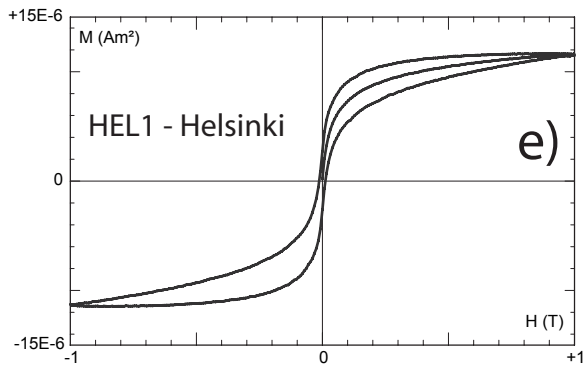
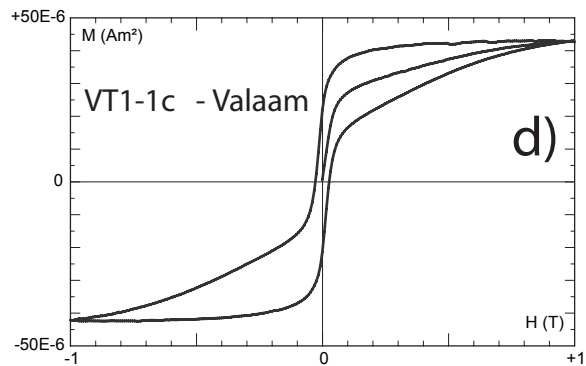
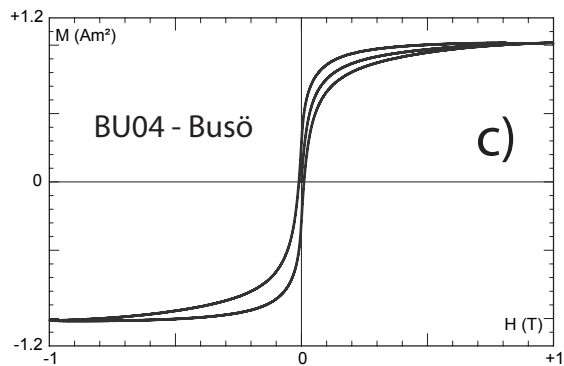
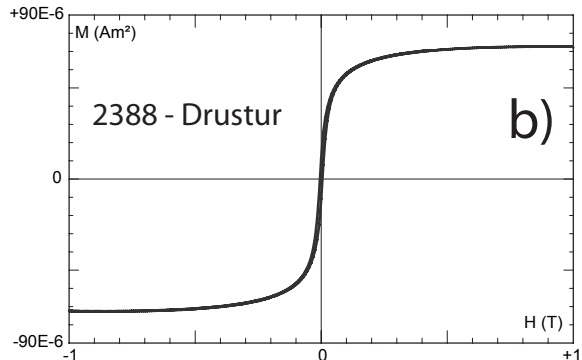
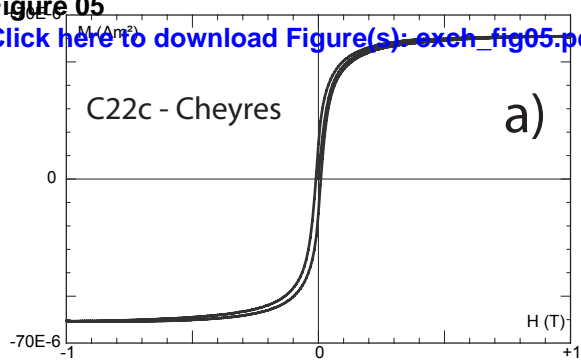
**Figure 05**[Click here to download Figure\(s\): exeh\\_fig05.pdf](#)

Figure 06

[Click here to download Figure\(s\): exch\\_fig06.pdf](#)

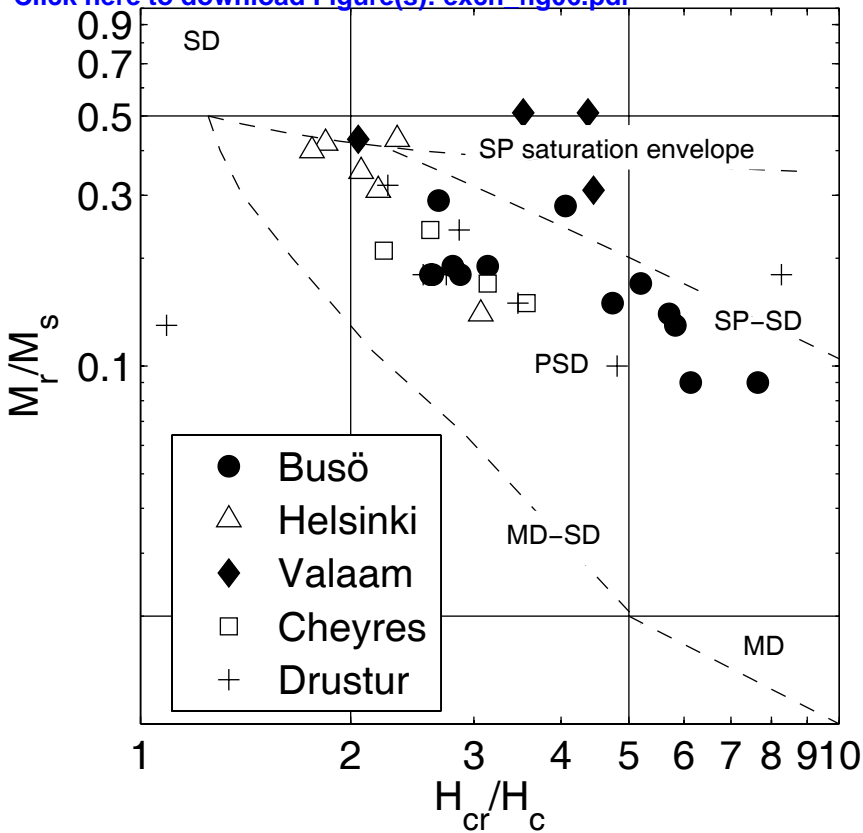
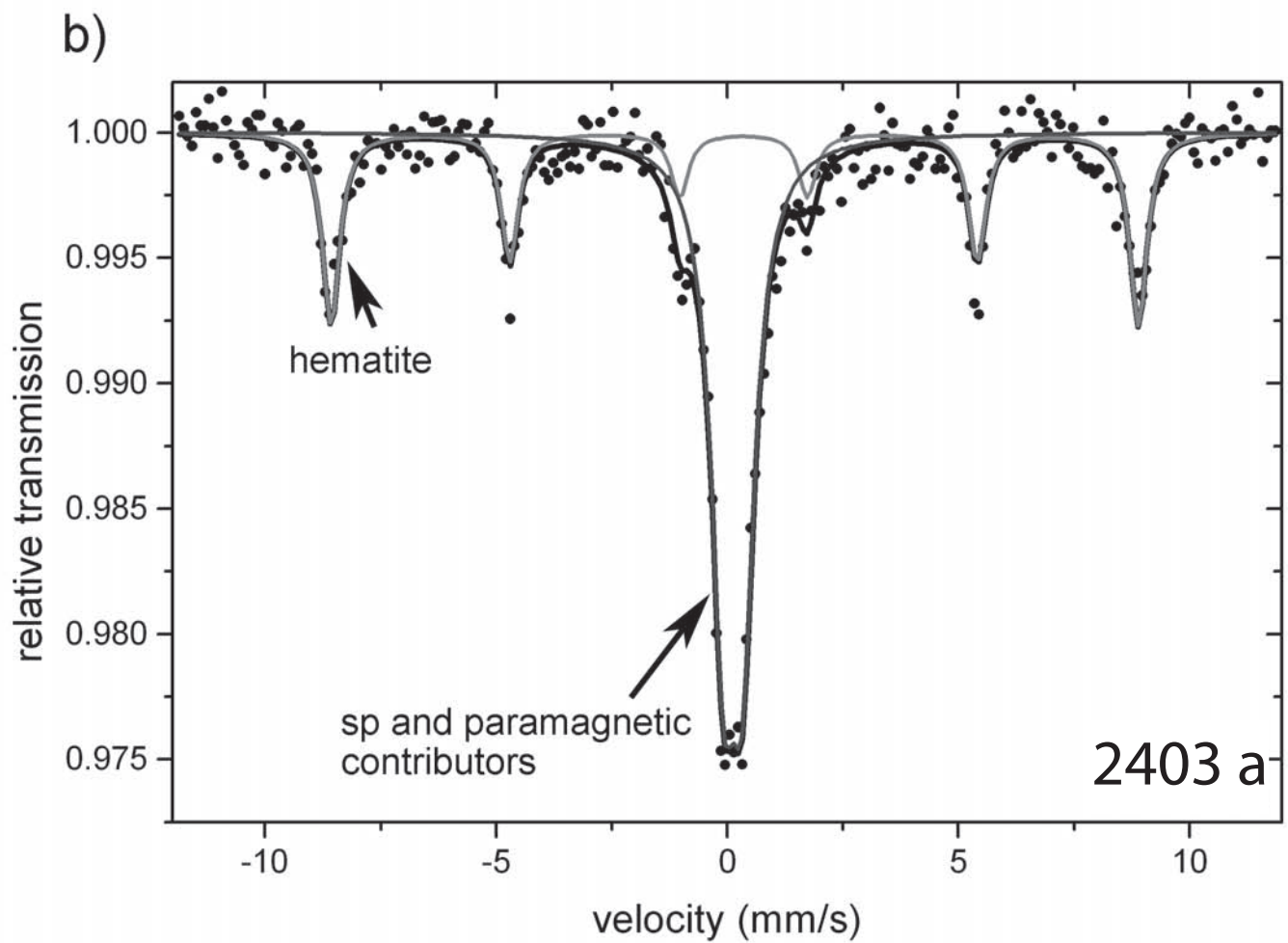
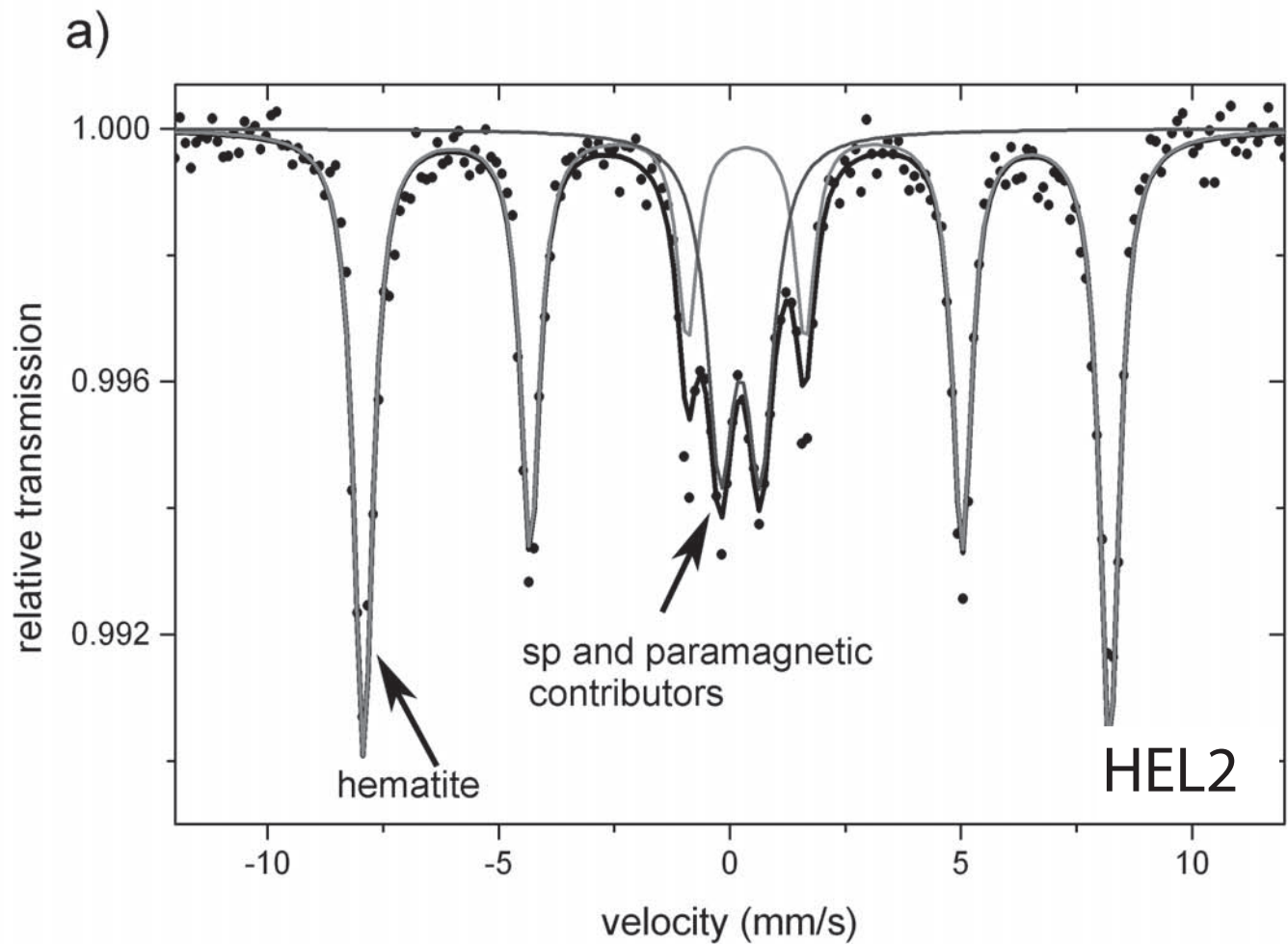


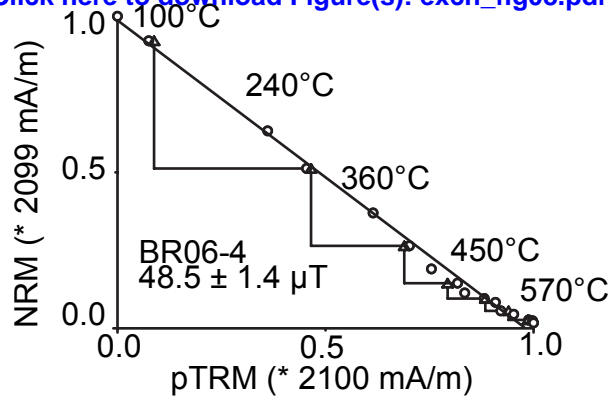
Figure 07

[Click here to download Figure\(s\): exch\\_fig07.pdf](#)

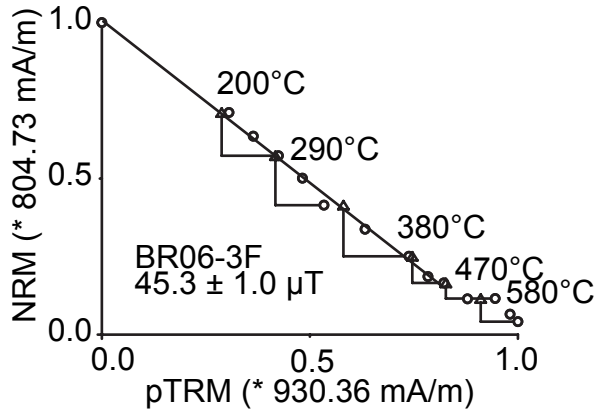


**Figure 08**

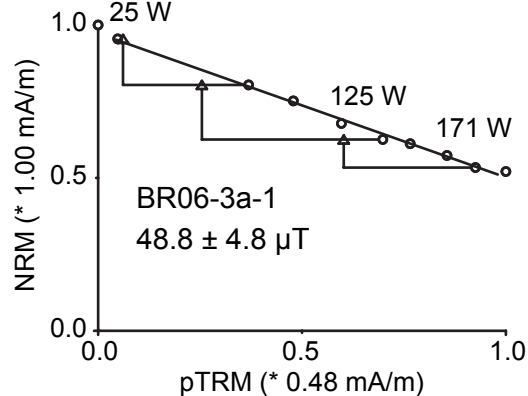
Helsinki, Coe

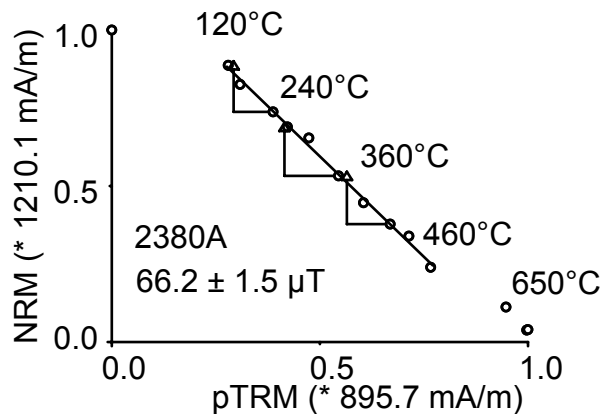
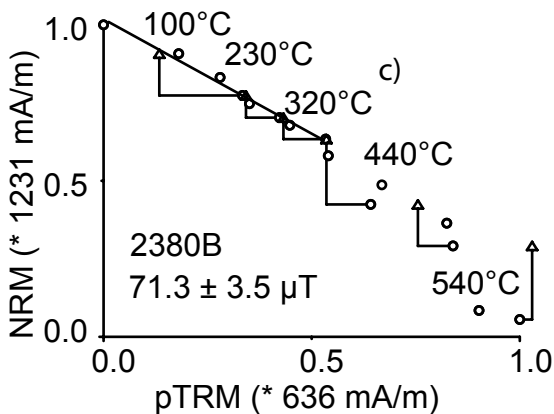
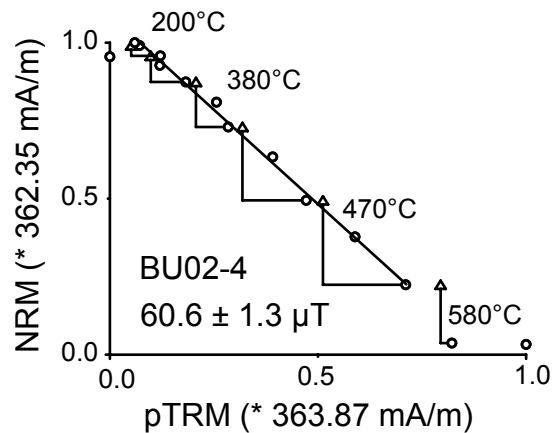
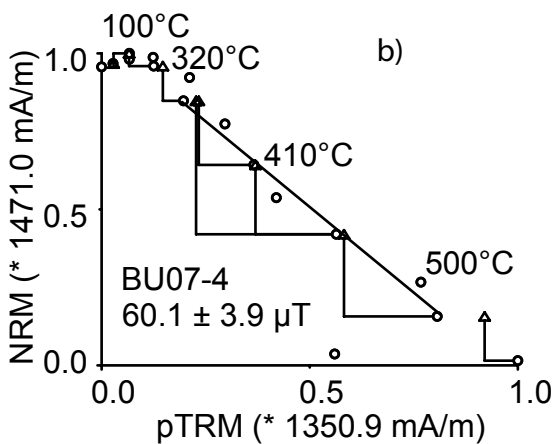
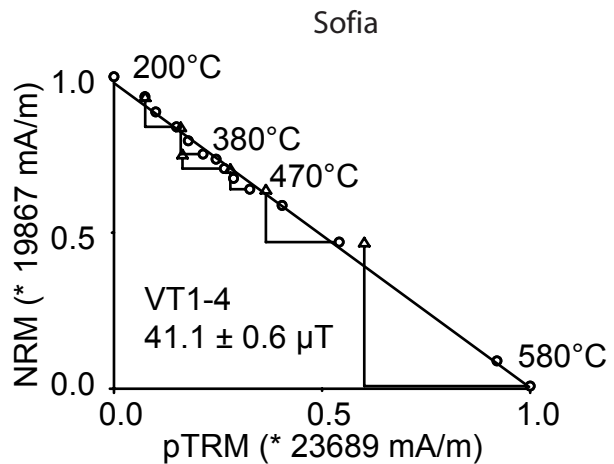
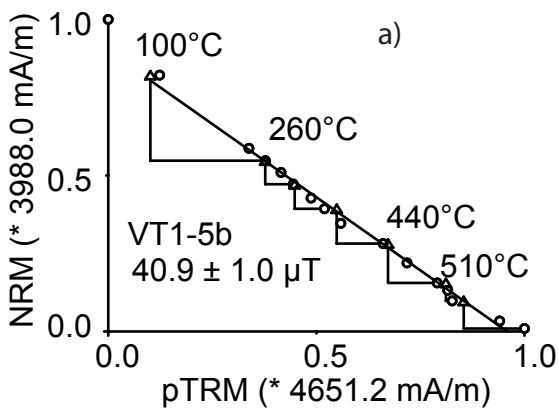
[Click here to download Figure\(s\): exch\\_fig08.pdf](#)

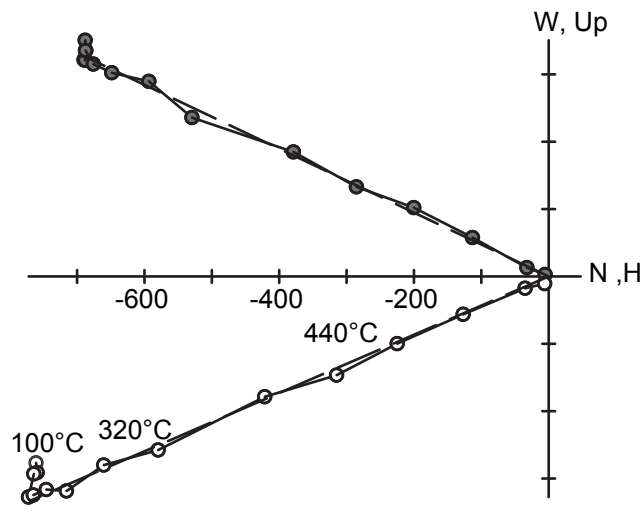
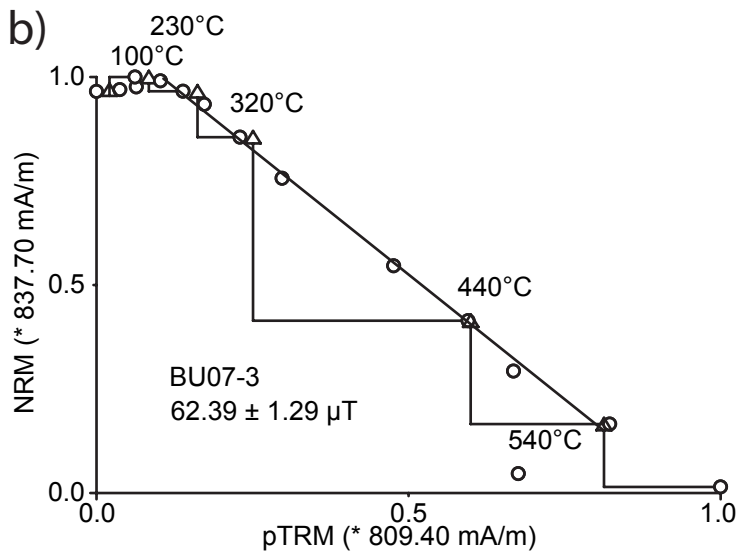
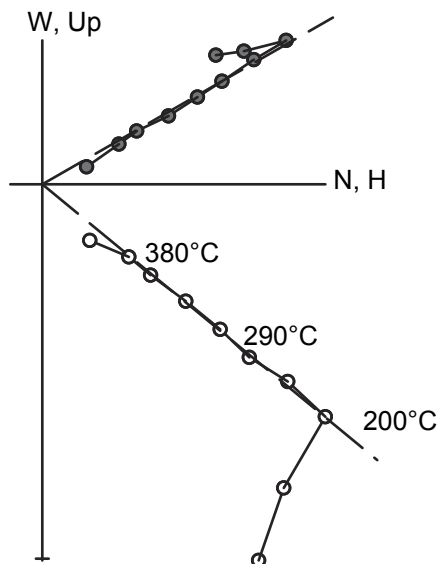
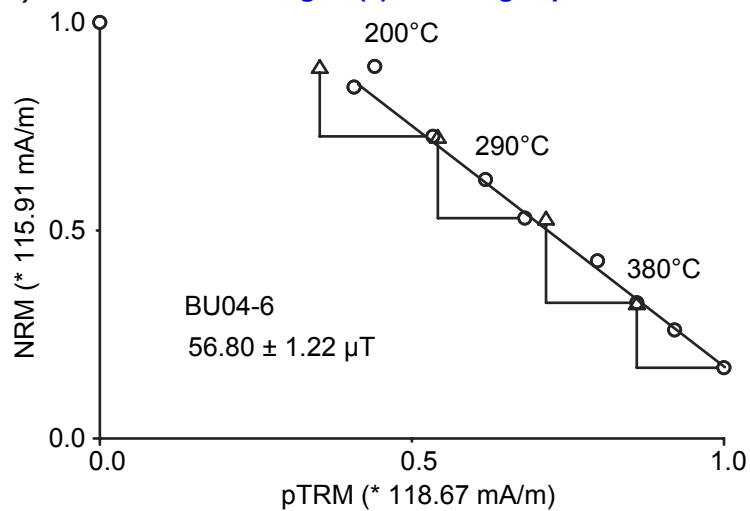
Sofia, Coe



Liverpool, microwave



**Figure 09**[Click here to download Figure\(s\): exch\\_fig09.pdf](#)

**Figure 10**[Click here to download Figure\(s\): \*\*exch\\_fig10.pdf\*\*](#)

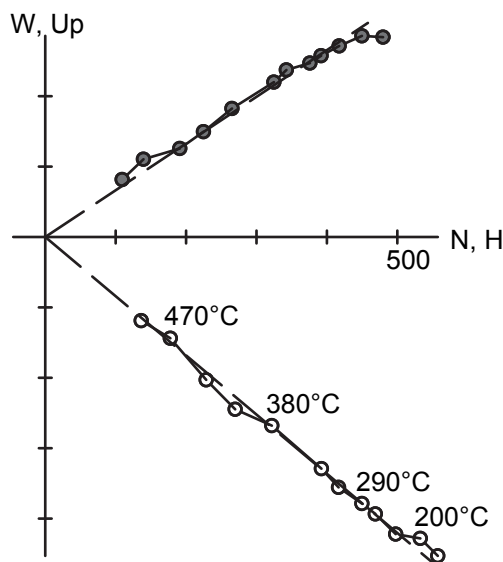
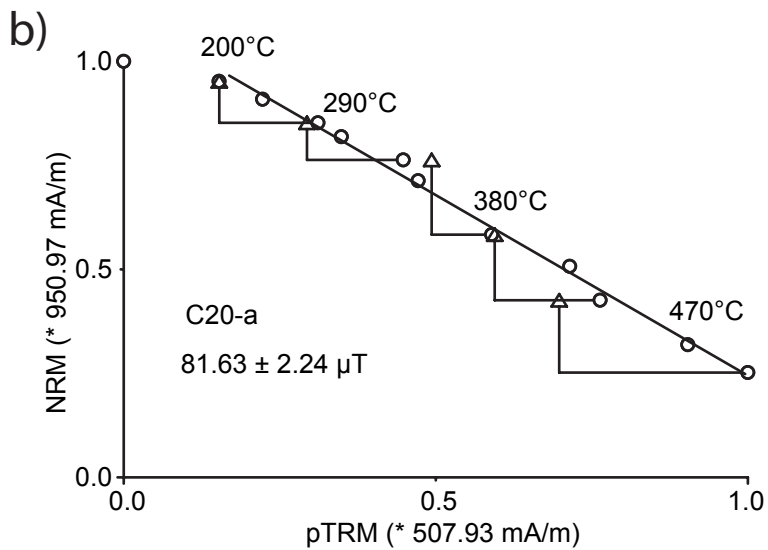
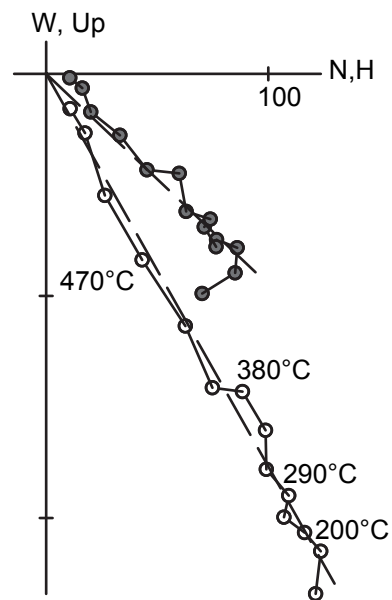
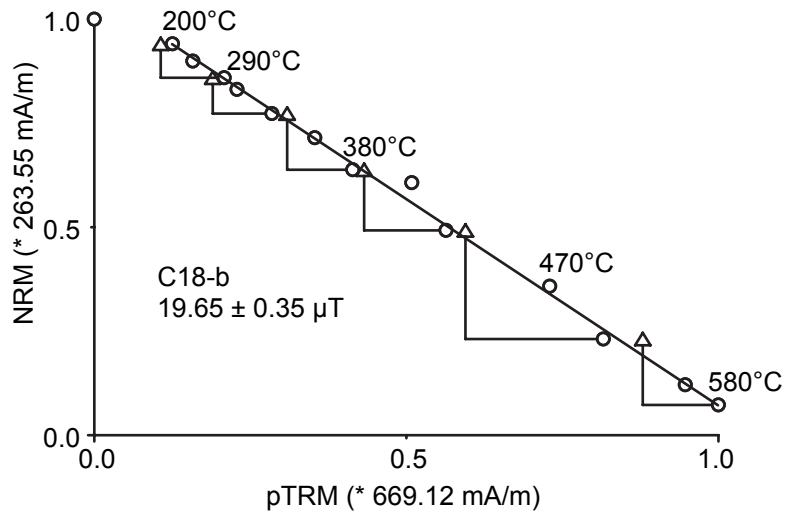
**Figure 11**[Click here to download Figure\(s\): `exch\_fig11.pdf`](#)



Figure 12

[Click here to download Figure \(C23b\) - virgin.pdf](#)

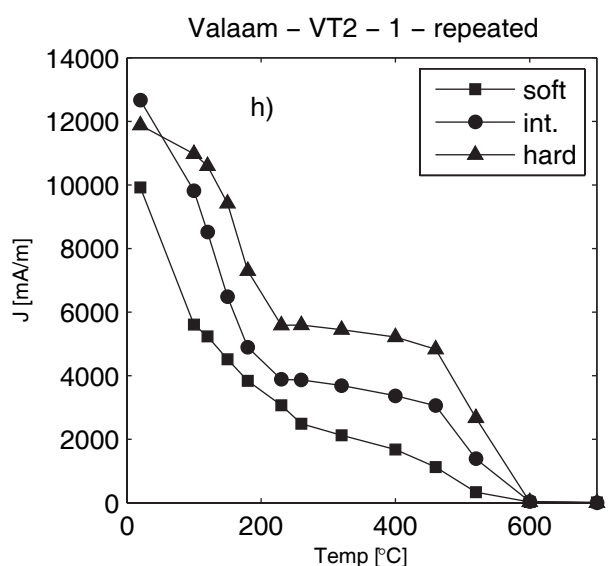
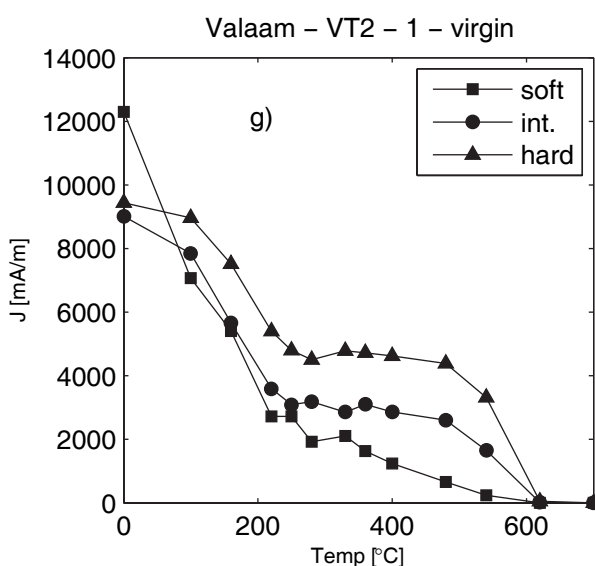
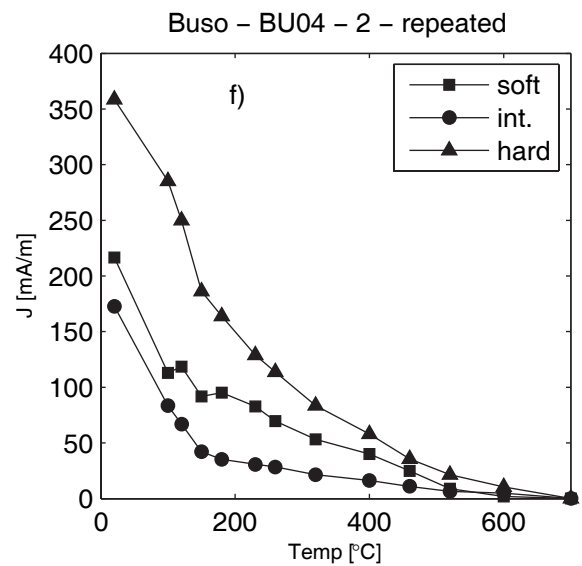
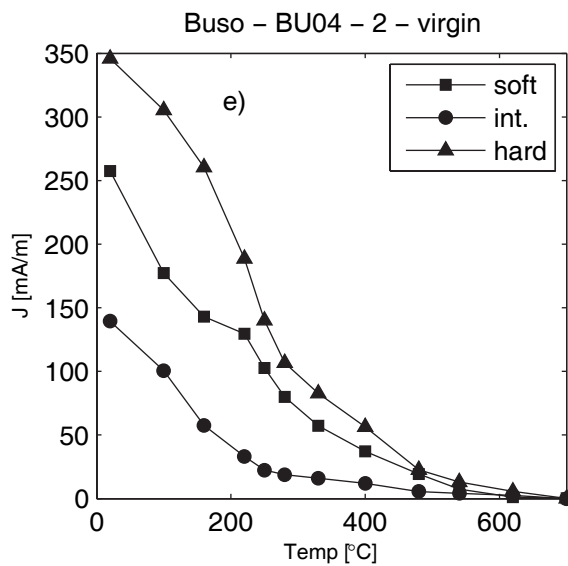
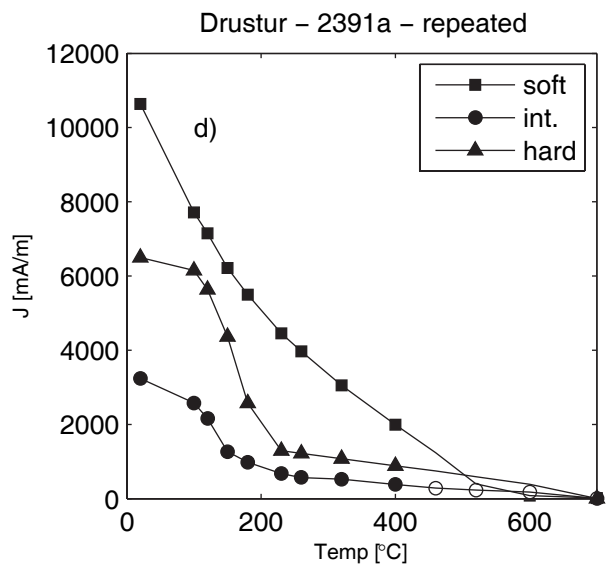
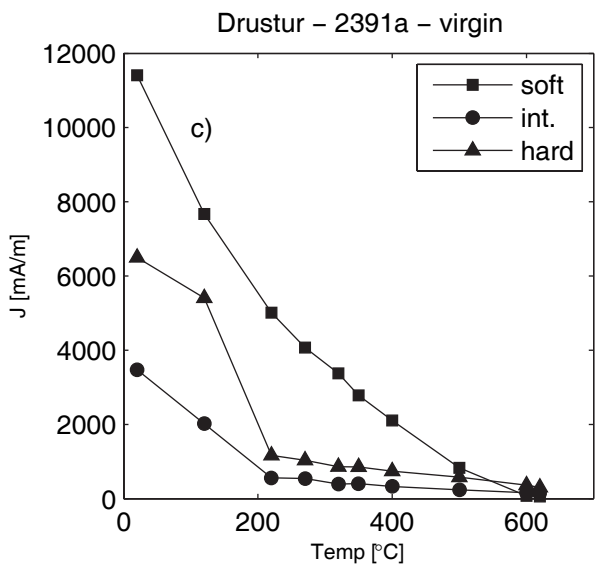
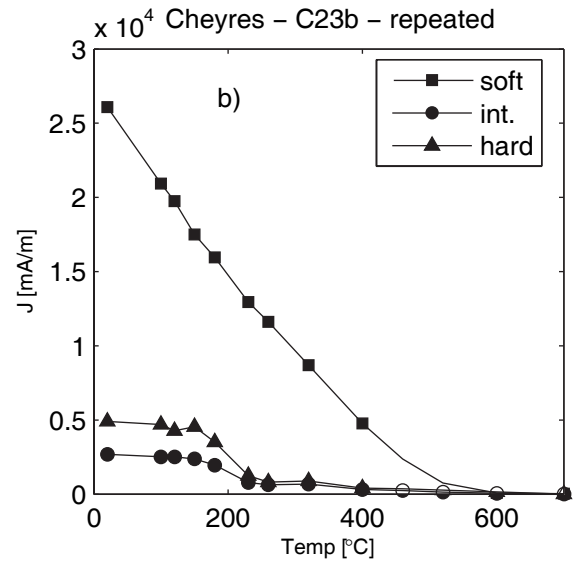
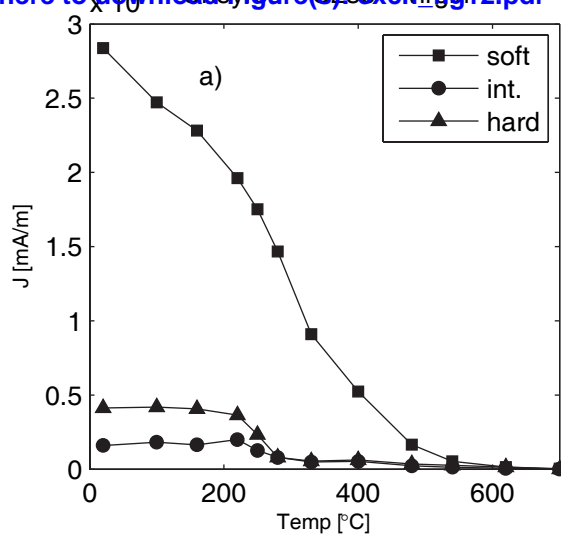


Figure 13

[Click here to download Figure\(s\): exch\\_fig\\_13.pdf](#)

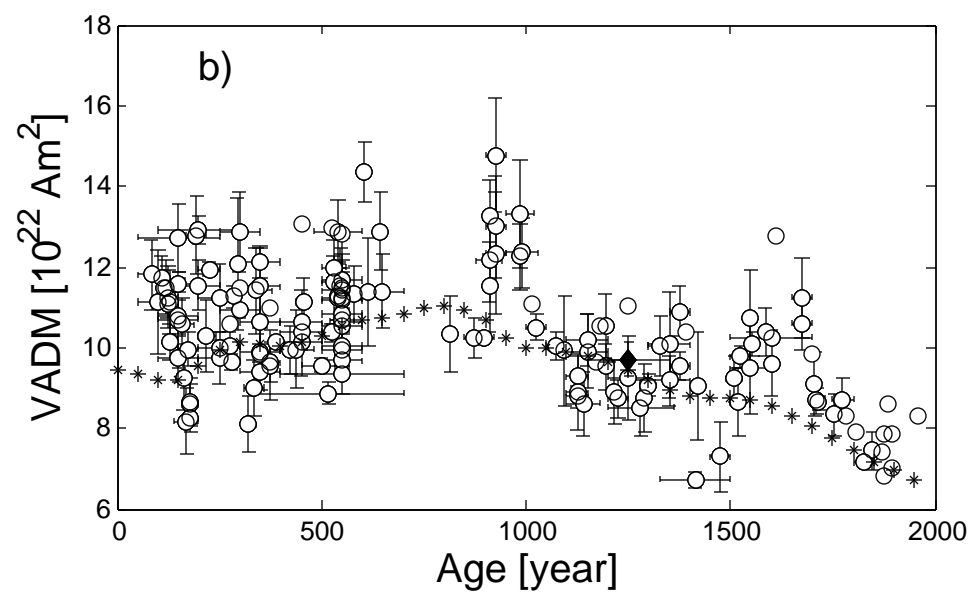
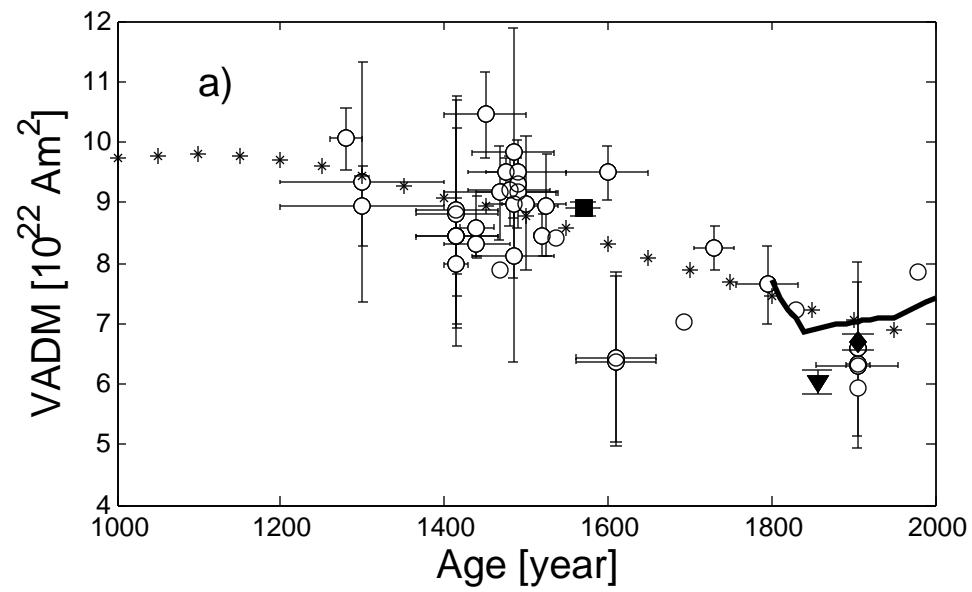


Table 01

exchange\_pap\_Table 1

Sample	Sv (%)	MDF (mT)	L-F test	soft	3IRM test int.	hard	HTK		SIRM test	Hc [mT]	Hcr [mT]	Mr/Ms	Hcr/Hc	Loop	Kfd [%]
							mineral	min. change							
<b>Cheyres, Switzerland (700 - 530 BC)</b>															
C04	5	18	0.16 / SD	540-620; 700	---	---			negative	8.1	29.1	0.15	3.57	N	
C06										10.4	23.1	0.21	2.23	N	
C15	6	24	0.32 / BM	360; 620	250; 330	250; 330	TM; M	not signif.	positive						
C16	5	18	0.22/ SD	480; 620	220	250			positive						
C19	6			400; > 620	220	270	M; MH	not signif.	positive						
C21	5	23	0.35/ BM	620	250	270			positive	6.1	19.3	0.17	3.14	N	
C22	8	24	0.29/ BM	620	250	250	TM; M	significant	negative	9.8	25.5	0.24	2.60	N	
C23	4	20	mixed	540; 620	270; 620	270; 620	TM; M	significant	negative						
<b>Drustur, Bulgaria (1200 - 1300 AD)</b>															
2380										8.0	66.1	0.18	8.27	W-W	7.5
2381	7	15	0.13/ SD	620	---	> 620	TM; M; H	significant	positive	7.6	21.6	0.24	2.86	N	11.0
2382	6			530	---	---			positive						10.0
2383							H	not signif.		4.7	16.2	0.15	3.47	N	8.0
2388							TM; M	no change							10.0
2390										8.6	19.5	0.32	2.26	N	10.0
2391	4	18	high coerc.	620	220; > 620	220; > 620			positive	5.8	6.3	0.13	1.09	W-W	10.0
2395	6	18	0.29/ BM	620	---	---			negative						10.0
2398	5	24	0.19/ SD	500; 580	220; 620	220; 620	TM	not signif.	positive						10.0
2400	4	41	0.10/ SD/mixed	400; 620	220	270; > 620	TM	not signif.	negative	5.5	26.2	0.10	4.81	N	8.4
2402	9			600	---	---	TM; M	not signif.		6.1	15.5	0.18	2.54	N	10.0
2403	4	30	- 0.97/ MD	540; 620	170; 620	220; 620			positive						
<b>Busö, Finland (1570 AD)</b>															
BU02		10.5	0.28 /BM	250; 620	340	340	TM; H	significant	positive	4.7	13.2	0.19	2.80	W-W	
BU03	4						TM; MH	significant		3.4	16.3	0.15	4.74	W-W	
BU04	8			220; 620	240; 700	250; 700	TM	not signif.	negative	10.2	41.3	0.28	4.06	W-W	
BU05		high	high coerc.	620	100; 620	200; 700	TM; H	significant	negative	5.1	16.0	0.19	3.14	N	
BU06	13			160; 250; 620	250; 620	250; 620	G; TM; H	moderate	negative	18.2	47.8	0.18	2.62	W-W	10.0
BU07	2	20	0.12/ SD	280; 620; 700	330; 700	330; 700	TM; M	significant	positive	5.4	15.5	0.18	2.87	N	
BU08	25						TM; MH	significant		7.1	40.7	0.14	5.71	W-W	
BU09	8						TM; H	significant		4.8	25.1	0.17	5.20	W-W	8.2; 10.1
BU10										4.3	24.9	0.13	5.83	W-W	
BU11	22			530; > 620	700	700			negative	4.4	26.9	0.09	6.13	W-W	
BU12										4.1	10.7	0.18	2.60	N	
BU13										32.6	249.0	0.09	7.65	W-W	
BU14										24.0	64.1	0.29	2.67	N	
<b>Valaam, Russian Karelia (1856 AD)</b>															

exchange\_pap\_Table 1

VT01							TM; H	significant		26.3	115.0	0.51	4.37	W-W	7.4
VT01-1	35	0.23 / BM	160; 540; 620	---	250				negative	27.4	96.8	0.51	3.53	W-W	
VT01-5a			520; 600	220; 600	220; 600										
VT02-1	high	high coerc.	280; 620	250; 620	250; 620	TM; M; H	significant			8.6	38.3	0.31	4.45	W-W	3.5
VT02-2			530; 620	260	180; 600				positive						
VT02a			580	180	180; 600	TM; H	not signif.			15.6	32.0	0.43	2.05	W-W	
<b>Helsinki, Finland (1906 AD)</b>															
BR06							TM; H	no change		17.5	40.8	0.43	2.33	W-W	
BR06-1f	2	35	high coerc.	480	160; 620	220; 620			positive	10.7	22.3	0.35	2.07	N	
BR06-2a	6	35	0.28 / BM	540	---	---	TM	not signif.	negative						
BR06-5a	1						TM	not signif.		10.9	24.0	0.31	2.19	N	8.0
HEL1a				180; 500	200; 500	200; 620	TM; H	not signif.		12.3	324.6	0.23	26.30	W-W	
HEL1b				110; 500	150; 500	200;500;680				7.1	21.9	0.14	3.07	W-W	
HEL2-6	5			100; 500; 580	100; 580	200; 700	TM; H	moderate		13.1	24.1	0.42	1.84	W-W	
HEL2-6f	2	30	high coerc.	280; 480	160; 540	220; 540	TM; H		positive	21.4	37.5	0.40	1.76	N	

Table 02

Sofia, Bulgaria										Helsinki, Finland										Liverpool, England							
Sample	B <sub>s</sub> [uT]	sB <sub>s</sub> [uT]	B <sub>L,ARM</sub> [uT]	sB <sub>L,AR</sub> M [uT]	Tmin	Tmax	q	f	w	Sample	B <sub>s</sub> [uT]	sB <sub>s</sub> [uT]	B <sub>L,AMS</sub> [uT]	sB <sub>L,AMS</sub> [uT]	Tmin	Tmax	q	f	w	Sample	B <sub>s</sub> [uT]	sB <sub>s</sub> [uT]	q	f	w		
<b>Helsinki, Finland (1906 AD)</b>																											
HEL2-2c	46.10	1.22	41.03	1.09	20	470	25.9	0.82	9.1	BR06-1b	40.29	1.56			100	600	21.6	0.97	6.9	BR06-3a-1	48.87	4.81	10.2	0.52	0.09		
HEL2-2d	45.19	1.13			20	580	34.5	0.99	10.0	BR06-2	54.04	0.86	52.42	0.83	20	570	53.9	0.98	14.4	BR06-3a-2	50.80	2.04	24.9	0.50	0.21		
HEL2-10f	44.18	0.88			20	440	27.2	0.71	9.6	BR06-2b	46.82	2.15			100	600	17.1	0.91	6.3	BR06-3a-3	50.74	7.27	7.0	0.33	0.04		
HEL2-11f	42.60	1.71	44.73	1.80	20	400	12.1	0.66	4.6	BR06-3b	53.96	1.35			20	400	26.8	0.82	10.9	BR06-3a-4	50.93	4.50	11.3	0.42	0.08		
BR06-3f	45.28	1.02	45.28	1.02	20	440	30.3	0.84	10.7	BR06-4	48.55	1.40	46.61	1.34	20	570	30.1	0.99	7.1	BR06-3a-6	49.09	3.29	14.9	0.47	0.12		
BR06-4f	45.75	2.39			20	440	12.8	0.83	4.5	HEL2-11a	52.69	1.72			20	400	17.3	0.70	7.0	BR06-3a-7	44.08	6.45	6.8	0.41	0.05		
BR06-5f	41.94	1.09	41.94	1.09	20	580	32.5	0.97	9.4	HEL1-1**	30.82	0.92			230	570	10.4	0.37	3.8	HEL2-12c-1	54.12	8.90	6.1	0.51	0.04		
HEL2-9f	42.59	1.00			20	410	22.4	0.71	8.5											HEL2-12c-5	50.00	7.01	7.1	0.43	0.05		
																				HEL2-12c-7	52.90	8.72	6.1	0.35	0.03		
<b>mean</b>	<b>44.20</b>	<b>1.62</b>									<b>49.38</b>	<b>5.35</b>								<b>49.92</b>	<b>1.09</b>						
w. mean s	44.08	0.29									50.91	4.26								50.25	0.84						
w. mean w	44.25	0.32									50.42	4.45								50.06	0.27						
<b>Valaam, Russian Karelia (1856 AD)</b>																											
VT1-4	41.14	0.68	41.55	0.69	20	580	49.1	0.99	14.1	VT1-2a	47.14	1.89			20	600	21.6	1.00	5.7								
VT1-5	41.42	1.83			20	580	16.7	0.85	4.8	VT1-5b	40.91	1.04			100	580	30.8	0.89	8.5								
VT2-3	43.93	2.33	43.93	2.33	200	580	8.3	0.50	2.5	VT2-2a	51.75	1.60	51.23	1.58	20	570	28.0	1.00	7.1								
										VT1-6a	41.93	0.83			20	600	46.0	1.00	12.3								
<b>mean</b>	<b>42.16</b>	<b>1.54</b>									<b>45.43</b>	<b>5.02</b>															
w. mean s	41.37	0.71									43.36	3.62															
w. mean w	41.53	0.88									44.63	4.24															
<b>Busö, Finland (1570 AD)</b>																											
BU02-1	67.65	2.65	69.00	2.70	200	500	17.5	0.80	5.8	BU02-7**	92.17	3.75	84.80	3.45	20	500	16.0	0.75	5.2								
BU02-4	60.58	1.31			200	500	28.6	0.72	9.6	BU07-3	62.39	1.29	61.77	1.28	230	500	30.4	0.75	11.5								
BU03-1	63.91	3.69			290	580	8.5	0.57	3.0	BU07-4	60.15	1.50	59.55	1.49	320	500	12.1	0.74	3.5								
BU03-2	62.57	3.05	73.83	3.60	260	440	8.7	0.51	3.9	BU10-1	68.23	3.21	64.14	3.02	200	500	13.9	0.73	4.6								
BU11-2**	44.88	4.44	44.88	4.44	320	540	4.4	0.51	1.8	BU11-1	60.38	2.18	59.78	2.16	100	500	17.3	0.70	5.2								
<b>mean</b>	<b>63.68</b>	<b>2.98</b>									<b>62.79</b>	<b>3.77</b>															
w. mean s	62.20	2.20									61.76	1.44															
w. mean w	63.21	2.75									62.74	2.58															
<b>Drustur, Bulgaria (1200-1300)</b>																											
2380a*	66.16	1.49			120	460	20.0	0.51	7.1	2380b	71.32	3.52	69.89	3.45	20	320	6.1	0.37	2.5	2391e-1	67.7	142.83	0.5	0.36	0.0004		
2380g	56.68	1.43	54.98	1.39	20	440	20.5	0.73	7.2	2388b	64.78	6.24	63.48	6.12	20	320	3.6	0.42	1.5	2391e-2	50.1	33.93	1.5	0.25	0.0035		
2380v	59.87	2.48	59.87	2.48	200	440	7.3	0.36	2.8	2390b	68.77	3.62			20	290	6.8	0.57	3.1	2391e-3	53.4	24.78	2.2	0.24	0.0063		
2388a*	61.20	0.91			20	460	50.5	0.84	16.8	2400g	60.53	4.62			20	320	6.1	0.37	2.5								
2388v	55.35	1.35			20	500	33.6	0.91	10.6	2403g	75.58	2.09	68.02	1.88	100	580	28.3	0.87	8.2								
2390g	52.77	1.71			20	320	14.9	0.63	7.5																		
2390v	52.54	1.04	55.17	1.09	20	440	37.8	0.88	13.3																		
2393b*	57.75	5.11			20	320	3.6	0.39	1.6																		
2396d	56.46	2.23	56.46	2.23	20	440	16.6	0.87	5.8																		
2402a	54.35	1.93			230	440	9.6	0.78	3.9																		
<b>mean</b>	<b>57.31</b>	<b>4.18</b>									<b>68.20</b>	<b>5.81</b>															
w. mean s	57.48	2.09									71.55	6.10															
w. mean w	57.27	1.98									70.77	7.28															
<b>Cheyres, Switzerland (700 - 530 BC)</b>																											
C01a	79.14	10.57			200	470	2.9	0.45	1.0	C04b	110.37	5.57	109.27	5.51	200	500	8.0	0.46	2.7								
C04a	92.43	6.13			100	440	5.4	0.42	1.9	C15c	25.82	1.38	26.08	1.39	200	500	9.4	0.57	3.1								
C18a	16.23	0.28			200	580	42.2	0.83	12.7	C22b	95.52	8.80	94.56	8.71	20	500	5.9	0.62	1.8								
C18b	19.65	0.35			200	580	41.2	0.82	12.4																		
C20a	81.63	2.24			200	500	20.8	0.64	6.9																		
<i>No result</i>																											

**Table 03**

Specimen number	pTRM		Outlier	Rock-magnetic properties evidence
	check (%)	tail check (%)		
HEL1-1b			X	HCSLT, two components
BR06-4a	8.5			BM; SIRM -
BR06-4b	8.8			BM; SIRM -
BU10-2	X	X		no linearity
BU11-2			X	SIRM -; SV=22%
BU04-6		21.4		HCSLT, two components
BU04-1	9.2			HCSLT, two components
BU02-7			X	HCSLT
2390a				no linearity; unstable direction
2396a	9			BM; SIRM -; mineral.change
C05		20		no linearity; unstable direction
C11		>15		no linearity; unstable direction
C16e	11.1			HCSLT, two comp.; mineral.ch.
C19d	8.3			HCSLT, sample broke
C21a	9			HCSLT-low contribution
C23a	10			SIRM -; HCSLT; mineral.change
C23e	8.1			SIRM -; HCSLT; mineral.change

